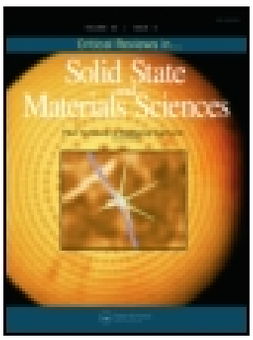

Critical Reviews in Solid State and Materials Sciences

ISSN: 1040-8436 (Print) 1547-6561 (Online) Journal homepage: http://www.tandfonline.com/loi/bsms20

Effect of Point and Line Defects on Mechanical and Thermal Properties of Graphene: A Review

G. Rajasekaran, Prarthana Narayanan & Avinash Parashar

To cite this article: G. Rajasekaran, Prarthana Narayanan & Avinash Parashar (2015): Effect of Point and Line Defects on Mechanical and Thermal Properties of Graphene: A Review, Critical Reviews in Solid State and Materials Sciences

To link to this article: http://dx.doi.org/10.1080/10408436.2015.1068160

Published online: 09 Oct 2015.

Critical Reviews in Solid State and Materials Sciences, 0:1–25, 2015

ISSN: 1040-8436 print / 1547-6561 online
DOI: 10.1080/10408436.2015.1068160

Taylor & Francis
Taylor & Francis Group

Effect of Point and Line Defects on Mechanical and Thermal Properties of Graphene: A Review

G. Rajasekaran, Prarthana Narayanan, and Avinash Parashar*
Department of Mechanical and Industrial Engineering, Indian Institute of Technology, Roorkee 247667, India

New materials with distinctive properties are arising and attracting the scientific community at regular intervals. Stiffness and strength are the important factors in determining stability and lifetime of any technological devices, but defects which are inevitable at the time of production can alter the structural properties of any engineering materials. Developing graphene with specific structural properties depends upon controlling these defects, either by removing or deliberately engineering atomic structure to gain or tailoring specific properties. In this article, a comprehensive review of defective graphene sheets with respect to its mechanical and thermal properties are presented and examined.

Keywords graphene, point defects, line defects, molecular dynamics, atomistic modeling, fracture toughness

Table of Contents

*E-mail: drap1fme@iitr.ac.in
Color versions of one or more of the figures in this article can be found online at www.tandfonline.com/bsms.

1. INTRODUCTION

Graphene is emerging as a potential candidate for developing nanocomposites with desired mechanical properties, thermal and electrical conductivities. Due to its exceptional mechanical properties, thermal and electrical conductivities graphene can also be used for more conventional purposes as compared to carbon nanotubes, which is still limited to aerospace applications. The unique properties of graphene sheet are tabulated in Table 1.

All these exceptional properties can be attributed to its two dimensional (2D) honeycomb space frame structure as illustrated in Figure 1.

Due to its exceptional properties, it has attracted increasing research effort for developing new engineering applications such as nano-actuators,[14–15] nano-sensors,[14,16] gigahertz oscillators,[14,17] drug deliverer,[14,18] field effect transistors (FET),[11,19–21] memory devices,[20] sensors, transparent conductive films, clean energy devices,[11] graphene field emission (FE), graphene-based gas and bio sensors,[22–27] tranparent electrodes, battery,[23,28] super capacitors,[28] electrical double layer capacitors (EDLCs),[28] pseudo capacitors,[28] graphene anodes, solar cells,[28] energy production and storage,[28–30] optoelectronic applications,[21] and room temperature humidity sensing applictions.[31] Researchers are also exploring the tribological properties of graphene.[32] In addition to these nanotechnologies, graphene is also listed among the top potential nanofillers for developing nanocomposites with improved mechanical properties and thermal and electrical conductivities.[14,20,28,33–37]

There is a wide spectrum of methods for the production of graphene sheets, which allow a flexibility of choices in terms of quality, production cost, size, and volume of production. Generally, graphene can be produced through top-down synthesis of graphene from micromechanical cleavage,[12,38–39] electrochemical exfoliation,[12,38] reduced graphene oxide,[12,38] exfoliation of graphite intercalation compounds,[12] arc discharge,[12] unzipping carbon nanotubes,[12] bottom-up synthesis of graphene from molecular precursors,[38] chemical vapor deposition (CVD),[38,40–42] chemical vapor deposition using catalytic metals,[38] CVD synthesis of graphene over nonmetals,[38] epitaxial growth of graphene on SiC,[38] and transfer to arbitrary substrates.[38] CVD techniques can be extended for commercialization (large-scale production). For more detailed information about various synthesis techniques the reader should refer to Refs.[11–12, 20–28, 30, 35–36, 39–71]

TABLE 1
List of properties for a single sheet of graphene

Property	Value
Young's modulus[1]	1.0 TPa
Fracture strength[1]	130 GPa
Tensile strength[2]	100 GPa
Thermal conductivity[3–4]	5000 w/mK
Shear modulus[5–6]	280 GPa
Longitudinal sound velocity[5,7–9]	20 km/s
Melting temperature [5,10]	4900 K
Specific surface area[11]	2630 m^2/g
Optical transmittance[12]	97.70%
High electron mobility[13]	250,000 cm^2/Vs

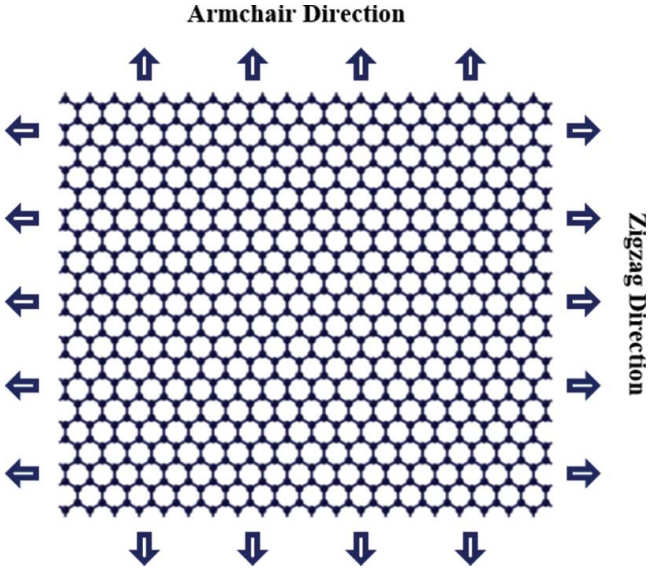

FIG. 1. Atomistic model of honeycomb space frame structure of graphene sheet.

1.1. Scope of the Review

Since the year 2004, when Novoselov et al.[64] published a path breaking results on the unusual eletronic properties of graphene sheet one can find exponantially increasing research and review publications in graphene over the past decade, as shown in Figure 2.

In 2007, Geim and his team[39] published a review on graphene entitle "The Rise of Graphene" which was the most frequently cited progress article for that year. Since than one can find many review articles on graphene with respect to synthesis methods,[11,20,40–42,48–49,72] physics of quantum hall effect,[48,72] characterization techniques, electronic structure,[40,48,72–73] and properties like magnetic, electrical and electromechanical, surface and sensor properties,[23,40] thermal properties,[47] and vibrational properties.[48] In the end of 2009, Geim[66] and Mazdak Taghioskoui[42] reviewed the major challenges in the field of graphene nanofillers and provided some basic knowledge about trends in graphene research. Another remarkable year in the field of graphene research was 2010, when Geim and Novoselov shared the Nobel Prize in physics for their outstanding groundbreaking work on graphene. After this historical event, researchers published more research and

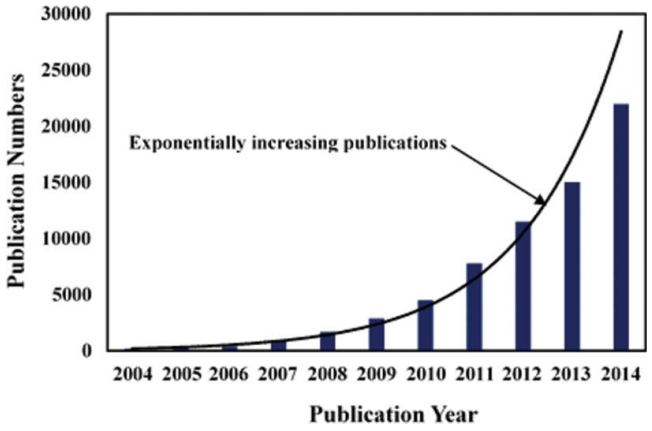

FIG. 2. Articles published in the period 2004–2014. (© Elsevier. Adapted with permission from Elsevier.[63] Permission to reuse must be obtained from the rightsholder.)

review articles on graphene.[11,12,20,21,23–28,30,35–37,46–65,74–77] Although, a greater number of review articles on different aspects of graphene such as synthesis, properties, and applications are published, there is, however, an opportunity to review defect engineering of graphene and their effect on the mechanical and thermal properties of graphene.

1.2. Importance of Graphene Defect Engineering

So far, most of the research on nanofillers is circumvent around its pristine form; however, structural defects which are inevitable during the production process[11,12,20–30,35,36,39–69] affect the mechanical properties as well as thermal and electrical conductivities[78] of graphene and graphene-based nanocomposites. Due to the method of production, chemical[79,80] and heat treatment,[81] as well as electron and ion beam irradiation,[82–85] it is hypothetical to obtain a pristine form of graphene.[78,86–87]

Investigating the effect of these defects on the mechanical properties, thermal and electrical conductivities of graphene are a key fact for the fundamental research in the field of nanofillers. Due to this reason, recently researchers diverted their research focus from exploring effect of defects on the mechanical and fracture properties of graphene. In 2015, Liu et al.[88] published a small-scale review on defects generation and healing in graphene. Production of graphene for different applications generally depends upon controlling these defects,[89] either by removing them or by intentionally engineering atomic structure to gain specific properties.[90–93]

Yadav et al.[94] investigated the effect of defect engineering for graphene by combining both Stone-Thrower-Wales (STW) and vacancy defects for improved hydrogen storage. Terrones et al.[95] provided an idea about defect control engineering-based tailoring of graphene's electronic, chemical, mechanical, and magnetic properties. Liu et al.[96] introduced dopant and STW defects to improve gas sensing properties of graphene.[97] In addition to studying the mechanical properties, fundamental understanding of the fracture mechanisms in graphene is not only scientifically interesting, but also practically important for preventing or controlling fracture in graphene.[98,99]

There are many studies on the mechanical properties and strength of pristine graphene carried out in the frame of molecular dynamics (MD), finite element, and experimental work. Studies on carbon nanotube (CNT), the rolled counterpart of graphene, suggest that the fracture in a honeycomb lattice of graphene may take two distinct[98,100–110] paths: brittle cleavage rupture or ductile failure by plastic flow instability. The activation of these two fracture mechanisms is mediated by temperature and loading rate. Because of the short-ranged covalent bonding between the sp^2 hybridized carbon atoms, the deformation of graphene generally involves the localized process of bond breaking or bond rotation whereas the sublimation by evaporation of carbon atoms can occur at high temperature.[98]

The aim of this article is to review the existing numerical techniques for simulating the mechanical, fracture, and thermal conductivity of graphene sheets in the presence of geometrical defects. An attempt has also been made by the authors to illustrate the challenges associated with the numerical modeling of defects in a monolayer of graphene.

2. NUMERICAL MODELING TECHNIQUES FOR GRAPHENE

As illustrated in Figure 3, experimental and numerical methods are commonly used techniques for characterizing different types of nanofillers. Atomic force microscope (AFM), scanning electron microscope (SEM), transmission electron microscope (TEM), X-ray diffraction (XRD) raman spectroscopy,[40] X-ray photoelectron spectroscopy, and near edge X-ray absorption fine structure spectroscopy[111] are widely used experimental techniques for characterizing nanofillers and nanocomposites. Nanofillers have the tendency to agglomerate under the influence of non-bonding attractive interaction, which ultimately limits the uniform dispersion of these nanofillers in matrix. Dispersion of nanofillers in matrix is still considered a challenging task in addition to cost and time

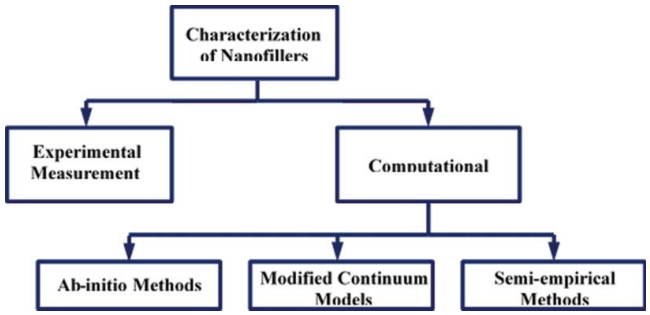

FIG. 3. Characterization of nanofillers.

involved in these types of experiments. These challenges motivate researchers to explore alternatives for characterizing these nanofillers and nanocomposites. Due to the tremendous improvement in the computational techniques, computational-based simulations are emerging as a better alternative for characterizing these nanofillers and nanocomposites. Computational models at the nanoscale can be classified in three subsections: ab-initio (First principal),[94,97,112–121] semi-empirical, and modified continuum models. Ab-initio approaches, such as the Hartee-Fock method and density functional theory (DFT), are more accurate, but are also considered highly computationally intensive.[8,82,94,122] Ab-initio techniques can be used for modeling nanostructures containing up to a few thousand atoms, whereas the structures, such as graphene, with thousands of atoms are normally considered as computationally intensive or inappropriate to be modeled with this method. A couple of continuum-based models, such as shell model and finite element-based models, are also employed by the researchers for characterizing the properties of nanostructures.[123-133] In addition to these continuum-based models, molecular mechanics-based finite element models are extensively used by the researchers for simulating mechanical properties and fracture behavior of nanofillers, such as CNT and graphene.[125,127,134–149] In finite element-based atomistic approach, bonded behavior between carbon-carbon atoms is simulated with the help of beam element and properties of these beam elements are derived from molecular mechanics.[82] Many attempts have been made by the researchers to improve the efficiency of these finite element-based atomistic models by incorporating different potentials for modeling the bonded interactions, but still these models are incapable of modeling the multi-physics problems that can be easily modeled in semi-empirical techniques. In order to reduce degrees of freedom, continuum-based models are computationally efficient but not as accurate as ab-initio and semi-empirical methods.

Semi-empirical methods, such as classical molecular dynamics (MD)[150–175] and tight-binding molecular dynamics (TBMD),[176,177] are considered less computationally intensive as compared to the ab-initio method, and are more accurate than the continuum-based approaches.[125,178] The details of the semi-empirical techniques, such as classical molecular dynamics, are covered in the following section.

2.1 Molecular Dynamics (MD)

Molecular dynamics is always considered a powerful tool for simulating biological molecules and chemical compounds.[178] For the last couple of years, application of molecular dynamics-based simulations has been extended to model the material properties of conventional as well as unconventional materials such as nanofillers and nanocomposites.[1,3,5,14,34,86,91,179–186] Entire success of any molecular dynamics-based simulation depends on the molecular potential opted for simulating the atomic interactions. A significant amount of progress has been made by the researchers in developing potentials for characterizing material properties for a range of materials. The principle of MD is to attain the force of each atom subjected by the interaction potential among the contiguous atoms. MD simulations follow the motion of all the atomic nuclei in the system by treating them as classical Newtonian particles[187] (because real systems of atoms at finite temperature are in constant motion) and integrating the equations of motion:

$$m_\alpha\left(\frac{d^2r}{dt^2}\right)_\alpha = -\frac{\partial U(r_1, r_2, \ldots\ldots r_N)}{\partial r_\alpha} = f_\alpha \quad \boldsymbol{\alpha} = \mathbf{1}\ldots\boldsymbol{N}, \quad (1)$$

where $\boldsymbol{N}$ is the number of atoms, $\boldsymbol{m_\alpha}$ is the mass of atom $\boldsymbol{\alpha}$, r_α is the position of atom α, and f_α is the time-dependent force acting on atom $\boldsymbol{\alpha}$ due to external effects and the presence of its neighbors, $(\boldsymbol{d^2 r/dt^2})$ is the acceleration of atom $\boldsymbol{\alpha}$ and $\boldsymbol{U}$ is the potential energy of the whole system.

There are three main steps in the MD-based simulation. Step one involves the evaluation of the potential energy and estimation of forces based on the current atomic positions and velocities. This is a modular component of the simulation, since any of the atomistic models can be used as the force model at this point.[178] For simulations with temperature control, the atomic forces are also modified by the thermostat algorithm during this step (most of the researchers are using Nose-Hoover[188–189] thermostat for modeling graphene).

In step two, the coordinates and velocities of the atoms are updated according to the integrator algorithm. According to the velocity-verlet (VV)[190] algorithm the coordinates and velocities of the atoms are updated as:

$$r(t_0 + \Delta t) = r(t_0) + v\left(t_0 + \frac{\Delta t}{2}\right)\Delta t \quad (2)$$

$$v(t_0 + \Delta t) = v\left(t_0 + \frac{\Delta t}{2}\right) + a(t_0)\Delta t \quad (3)$$

where $\boldsymbol{r}$, $\boldsymbol{v}$, and $\boldsymbol{a}$ are the position, velocity, and acceleration of an atom, respectively; $\boldsymbol{t_0}$ is the initial time, $\boldsymbol{\Delta t}$ is the time step. For constant stress simulations, the shape and size of the simulation box may also be updated during this step. In order to obtain stress-strain ($\boldsymbol{\sigma}$-$\boldsymbol{\varepsilon}$) curves, one can use the following virial stress equation[191,192] to estimate atomic stress of individual atoms during deformation:

$$\sigma_{ij}^{\alpha} = \frac{1}{\Omega^{\alpha}}\left(\frac{1}{2}m^{\alpha}v_i^{\alpha}v_j^{\alpha} + \sum_{\beta=1,n} r_{\alpha\beta}^{j} f_{\alpha\beta}^{i}\right), \quad (4)$$

where $\boldsymbol{i}$ and $\boldsymbol{j}$ denote indices in Cartesian coordinate system; $\boldsymbol{\alpha}$ and $\boldsymbol{\beta}$ are the atomic indices; $\boldsymbol{m^{\alpha}}$ and $\boldsymbol{v^{\alpha}}$ are mass and velocity of atom $\boldsymbol{\alpha}$; $r_{\boldsymbol{\alpha\beta}}$ is the distance between atoms $\boldsymbol{\alpha}$ and $\boldsymbol{\beta}$; and $\Omega^{\boldsymbol{\alpha}}$ is the atomic volume of atom $\boldsymbol{\alpha}$. The atomic volume can be

taken from the relaxed graphene sheet with a thickness of 0.34 nm.[191,193] Similarly, thermal conductivity (k) of the simulated atomic configuration can be estimated by using the following equations:

$$k = \frac{J}{2A\left(\frac{\partial T}{\partial x}\right)} \tag{5}$$

$$J = \frac{\sum N_{transfer}\left(m_h v_h^2 - m_c v_c^2\right)0.5}{t_{transfer}} \tag{6}$$

where ${}^{\partial}T/_{\partial}x$ is temperature gradient along the heat flux direction, $\boldsymbol{A}$ is cross sectional area, $\boldsymbol{J}$ is the heat flux, $\boldsymbol{t_{transfer}}$ and $\boldsymbol{N_{transfer}}$ are summation time and number of exchange, respectively, and $\boldsymbol{h}$ and $\boldsymbol{c}$ refer to hot and cold atoms, respectively.

Finally, step three provides the useful output from the simulation. This may involve collection of statistical data (for time averages of temperature, pressure, etc.) or the writing of atomic trajectories for post processing and visualization. Young's modulus (E), fracture strength (σ_f), and fracture strain (ε_f) can be derived from the simulated σ-ε curves; the Young's modulus value can be calculated as the initial slope of the σ-ε curves.[191]

2.1.1. Interatomic Potentials

Interatomic potentials employed in MD-based simulations are a mathematical description of the potential energy of the atomic system. The goal of interatomic potentials or force fields is to give numerical or analytical expressions that can estimate the energy landscape of a large atomic system. As stated earlier, entire success of any atomistic simulation depends on the interatomic potential employed for simulating the bonded and non-bonded interaction between the atoms. It is desired that the potential accurately reproduces the mechanical, fracture, and thermal characteristics of the material under consideration. Most of the potentials employed in atomistic simulations of metals, nanofillers, and nanocomposites have been empirically devised and validated against either experimentally or higher fidelity modeling data.[178]

A variety of interatomic potentials or force fields have been developed, ranging through different levels of accuracy and complexity and the simplest form of atom-atom interaction is pair potential, the potential energy of which only depends on the distance between two particles. The total energy of the system is given by summing the energy of all atomic bonds over all $\boldsymbol{\alpha}$ particles in the system. The general form of potential energy for a set of atoms is given by:

$$U_{total} = \frac{1}{2}\sum_{\alpha=\beta=1}^{N}\sum_{\beta=1}^{N}\phi\left(r_{\alpha\beta}\right) \tag{7}$$

where $r_{\alpha\beta}$ is the distance between particles $\boldsymbol{\alpha}$ and $\boldsymbol{\beta}$ and $\phi\left(r_{\alpha\beta}\right)$ is the potential energy between particles $\boldsymbol{\alpha}$ and $\boldsymbol{\beta}$. Generally, symmetric and ordered structures of carbon-based nanofillers (e.g., CNT's, graphene) can be modeled using the cluster potentials such as CHARMM or AMBER, but these potentials have limited application and cannot be employed for modeling bond breaking.[178] As this limitation is quite severe, it is more common to use the Tersoff-Brenner potential for simulating the bond breaking and formation in carbon-based nanofillers.[178] More transferable behavior can be obtained with the more costly tight-binding (TB) or tight binding-bond order potentials (TB-BOP) approaches, or with the more recently developed reactive force-field (ReaxFF) model.[178]

Researchers are extensively using Morse potential, reactive empirical bond order (REBO) potential,[194] and, most recently, introduced adaptive intermolecular reactive empirical bond order (AIREBO) potential[195] for simulating and characterizing the mechanical properties, thermal conductivity, and fracture behavior of CNT and graphene. As compared to other potentials, Morse is a two-body potential; hence, its accuracy is limited with large systems such as graphene and CNT. AIREBO potential is an improved form of REBO potential, which includes a component for non-bonded interactions and one more component for four body torsional interactions. Usually four-body torsional term is considered important while modeling the curved structures such as CNT. Bonded interactions are considered to be primarily responsible for maintaining the structural strength of carbon based nanofillers, but in large systems such as graphene these non-bonded interactions also have significant contribution in imparting strength to the structures. Mathematically AIREBO potential is defined as:

$$E^{AIREBO} = \frac{1}{2}\sum_{i}\sum_{j\neq i}\left[E_{ij}^{REBO} + E_{ij}^{LJ} + \sum_{k\neq i,j}\sum_{l\neq i,j,k}E_{kij}^{ltors}\right], \tag{8}$$

where $\boldsymbol{i,j,k}$ and $\boldsymbol{l}$ refers to individual atoms, $\boldsymbol{E}$ is the total potential energy, E_{ij}^{LJ} is the component representing non-bonded Lennard Jones potential, E_{kij}^{ltors} represents the four-body torsional term in AIREBO, and E_{ij}^{REBO} is the REBO potential. REBO potential consists of attractive and repulsive terms, as described below in Eq. 9):

$$E_{ij}^{REBO} = f(r_{ij})\left(E_{ij}^{\text{Repulsive}} + b_{ij}E_{ij}^{\text{Attractive}}\right), \tag{9}$$

where b_{ij} is the bond order which regulates the bond strength, $f(r_{ij})$ is the cut off function. Cut off function limits the bonded interaction between the nearest neighboring atoms lying within the cut off distance.

2.1.2. Cut-off Radius

A basic assumption in the development of many interatomic potential is that atomic interactions are inherently local, the idea is that beyond some bond length atoms interact so weakly that they make essentially no contribution to the

total energy. To be consistent with this view, the interatomic potential energy function must be constructed in such a way that the energy contribution due to a given atom is only affected by atoms within a specified distance called cut-off radius and denoted by r_{cut}. A smaller value for cut-off radius improves the computational efficiency, but on the other hand it reduces the accuracy of the simulations, hence cut-off radius is usually defined in such a way that accuracy of the calculations will not be affected.

To investigate the effect of defects in graphene, Wu and Wei[197] used a value of 1.92Å, while Jhon et al.[198] used the value of 2.0Å as the C-C bond cut off radius in order to avoid unphysical results before the bond breaking. In order to study the effect of cut-off radius on the tensile strength of graphene, different cut-off radius used in different research works is compiled in Figure 4. It can be inferred from the trend shown in Figure 4 that tensile strength of graphene continuously decreases with an increase in cut off radius from 1.75–1.92 Å.[196] It can also be inferred from the data plotted in the same figure that estimated value of tensile strength is almost constant for the value of cut-off radius higher than 1.92 Å.[196]

Inflection point is defined as the value of strain at which bond breaking takes place, cut-off radius smaller than this point has spurious effects on the estimated tensile strength, whereas a higher value usually have no impact on the estimated tensile strength.[196]

3. DEFECTS IN GRAPHENE

So far, most of the research progress made in the field of graphene is with respect to its pristine form, but recently it has been established that different productions techniques exposed pristine form of graphene to different type of defects. As discussed earlier in this article, imperfection is generally introduced in the graphene sheets, due to different methods of production,[22,44,70,112–118,144,154–176,199–204] chemical treatment,[79,205] and irradiation.[83–85,206,207] The mechanical, thermal, and fracture properties of graphene are extremely susceptible to lattice imperfections. Defects in a graphene sheet can be classified as intrinsic (inbound defects)[97] and extrinsic defects (presence of foreign particles). Defects in the graphene can also classified as point defects (e.g., vacancy, as atoms, interstitials, and Stone-Thrower-Wales defect) and line defects (e.g., dislocations and grain boundaries). In this article, effect of these defects has been elucidated with respect to their impact on the mechanical properties, thermal conductivity, and fracture properties of single sheet of graphene.

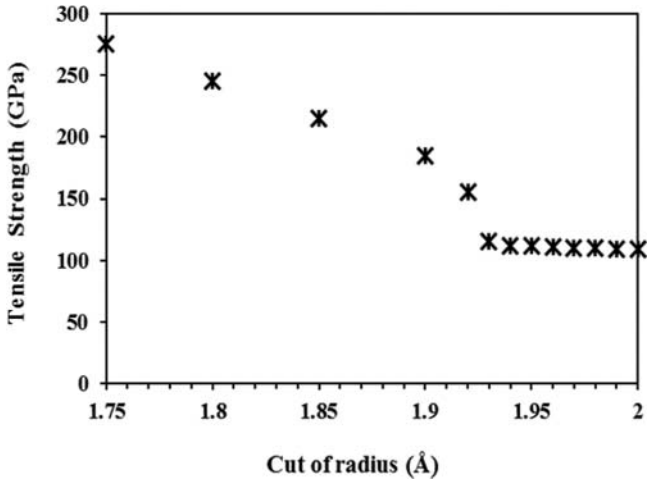

FIG. 4. Relationship between simulated tensile strength and C-C bond cut-off radius (© Elsevier. Adapted with permission from Elsevier.[196] Permission to reuse must be obtained from the rightsholder.)

3.1 Pristine Form of Graphene

Stiffness is considered the most measured mechanical property of any material system. Before discussing the effect of defects on the mechanical properties, thermal conductivity, and fracture behavior of graphene, an overview is provided about common properties of a pristine form of graphene. Lee et al.[208] experimentally investigated the elastic properties of pristine form of graphene and reported the value of Young's modulus as 1 ± 0.1TPa which is generally considered as the most commonly used value of Young's modulus for graphene. Frank et al.[209] used the atomic force microscopy- (AFM) based direct approach for obtaining the mechanical properties of atomically thin sheets of graphene and the same technique had also been used by Rasuli et al.[203] to estimate mechanical properties of few-layer thick graphene cantilever. Suk et al.[204] also used AFM-based techniques to determine mechanical properties of graphene and the results were validated with the finite element-based models. Zhang et al.[199] simultaneously determined mechanical property and number of graphene layers using instrumented nano-indenter. In their research work,[199] a linear relationship between the number of layers and hardness of graphene was reported. Navarro et al.[202] used tip-induced deformation experiment for determining elastic properties of chemically derived single graphene sheet.

On the other hand, numerical based techniques had been employed by Shen et al.[210] for investigating the effect of temperature and dimensions of graphene on the Young's modulus. Shen and his research team employed molecular dynamics-based simulations to study the effect of aspect ratio of graphene on the elastic properties of graphene. It was finally reported in their research work that Young's modulus of graphene is a size- and temperature-dependent property. It was concluded in their research work that Young's modulus decreases with increase in temperature and shear modulus was reported weakly dependent on the temperature.

The results published by Shen et al.[210] was found to be in accordance with the earlier published results of Jiang et al.[179] and also Jiang et al. estimated the Young's modulus of graphene with respect to size of graphene and simulation temperature. It was reported in their molecular dynamics-based

research article[179] that Young's modulus of graphene usually increases with the increase in the size of the sheet, but value is saturated after a threshold size of the graphene sheet. The trend for Young's modulus with respect to temperature reported in the research article[179] was contrary to the one reported in Shen et al.[210]

In 2010, Tsai and Tu[180] performed a molecular dynamics-based study on single layer of graphene sheet and graphite flakes. They performed the molecular dynamics-based simulation with two different types of ensembles, and concluded that modified NPT ensemble (Constant number of atoms, pressure and temperature of simulation box) has a better accuracy for simulating the mechanical behavior of graphene, as compared to conventional NVT (number of atoms, volume of simulation box, temperature of simulation) ensemble. In addition to this, it was also reported in Tu[180] that mono-layers of graphene has better reinforcing properties than the graphite flakes.

Ni et al.[182] also studied the elastic properties of graphene sheet with the help of molecular dynamics based simulations. In their research work, elastic properties and fracture behavior of graphene was simulated with respect to the direction of loading. It can be inferred from the numerical modeling results of Ni and his research team that graphene has higher strength while loading along direction aligned with the bond direction (longitudinal direction). The same conclusion was aslo made by Parashar et al.[211] in their numerical simulation to study buckling strength of graphene. In addition to tensile loading, molecular dynamics-based modeling was also performed to simulate the double-clamped bending experiment with the single layer of graphene.[212] In that work with bending, the relationship between the centerline deflection and concentrated forces has been derived from molecular dynamics in conjunction with the continuum theory. In their continuum-based approach, Reddy et al.[213] discussed the importance of energy minimization with respect to different elastic properties. In addition to molecular dynamics, finite element-based approach has also been employed by many researchers for estimating elastic properties of graphene.[123,125,210,214–221].

Young's modulus of pristine graphene estimated by different researchers is compiled in Figure 5. The large deviation in Young's modulus ranging from 0.80–1.367 TPa is attributed to different measurement techniques, simulation methods, types of boundary conditions (temperature range, types of loading, directions of loading, size, number of layers, and types of potential used), however the mean value of Young's modulus is $\sim$ 1.041 TPa.

Resistance to crack propagation or fracture toughness is undoubtedly also among the important properties for structural materials. In a stressed component fracture by brittle cleavage or ductile rupture is determined by the competition between bond-breaking[230] at the crack tip and plastic deformation and/or bond rotation in the surrounding area of the crack. The crack initiation in graphene sheet is accompanied by the breaking down of the carbon-carbon bonding. Once the crack is initiated, it will quickly propagate through the whole graphene sheet even without being stretched, indicating the crack propagation in graphene is a spontaneous process.[86] Dynamic and static fracture properties of graphene sheet and CNT, which is suitable for nanocomposites at high strain rate impact loading, were studied using modified Morse potential in Niaki et al.[231] In Niaki et al.[231] it was concluded that the dynamic fracture is dependent on nanostructure size and independent of strain-rate.

The fracture properties of single-layer graphene sheet estimated by different researchers in both armchair and zigzag directions are illustrated in Figures 6 and 7, respectively.

In addition to exploring the mechanical properties, researchers are also keeping their focus on exploring the

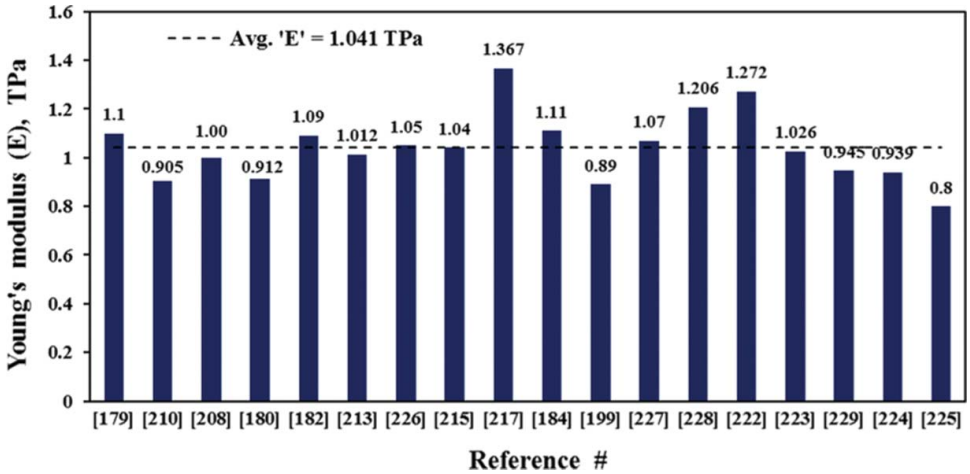

FIG. 5. Young's modulus of pristine graphene. Molecular Dynamics - [179, 180, 182, 184, 210, 222–225], Experiments - [199, 208, 225], Continuum Mechanics - [213, 215, 224], Density Functional Theory (DFT) - [226–228], and Finite Element Method - [217, 229].

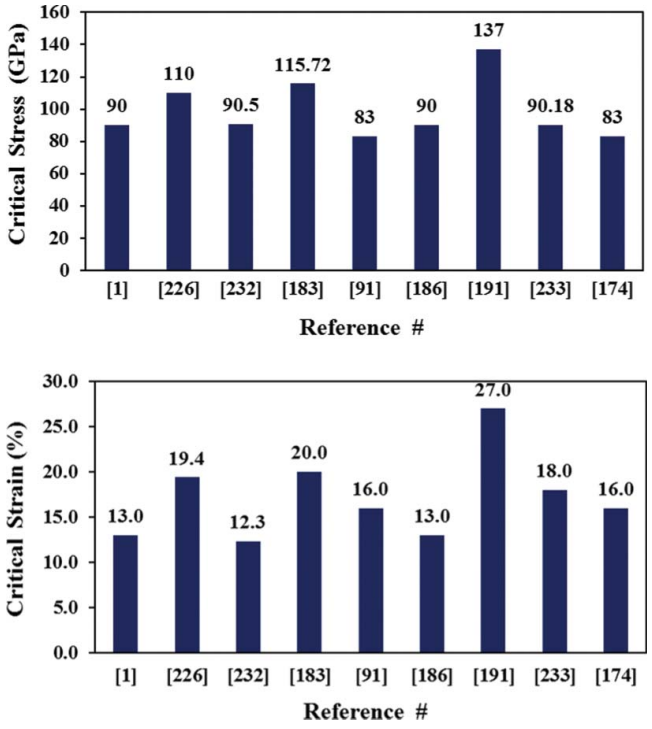

FIG. 6. Critical stress and strain of pristine graphene in Armchair direction. Molecular Dynamics - [1, 91, 174, 183, 186, 191], Quantum Mechanics - [226, 232], and Structural Mechanics [233].

thermal properties of graphene and the effective ways to modulate its thermal conductivity.[235–244] Due to sp2 bonding between the carbon atoms in graphene, it has extremely high in plane thermal conductivity of 2000–4000 W/mK at room temperature.[245] The upper limit corresponds to isotopically purified graphene with large grain sizes,[246–248] whereas the lower bound corresponds to isotopically mixed sample or graphene with small grain size. Any naturally occurred disorder or foreign particle in the lattice of graphene leads to more phonon scattering and lower the values of thermal conductivity. In pristine graphene, phonon scattering or dispersion from the edges leads to the modulation of thermal conductivity.[249] Generally, Umklapp and edge scattering are more common scattering phenomenon in single sheets of graphene. It was reported in the research work of Yang et al.[249] that Umklapp scattering is negligible if graphene nano ribbon length is smaller than the phonon mean free path (<775 nm). In small size graphene sheets (<775 nm) edge scattering dominated the scattering mechanism. It was concluded in the same article[249] that the shorter the ribbons the stronger the edge scattering will be. Edge scattering phenomenon in shorter graphene ribbons will lead to reduction in thermal conductivity. The boundary scattering will be weakened with increased ribbon width. However, the increased number of phonons and the smaller energy separation between phonon modes promote the probability of Umklapp scattering in wider graphene nanoribbons.

3.2. Effect of Defects on Graphene

This section elucidates the effect of different types of defects on the mechanical properties, thermal conductivity and fracture behavior of graphene. During the last couple of years, a significant amount of contribution has been made in the field of modeling these defects for a single layer of graphene sheet. This article updates the current state of art in simulating the effect of these defects on the single layer of graphene sheet.

3.2.1. Stone-Thrower-Wales (STW) Defects

One of the unique properties of the graphene lattice is its ability to reconstruct by forming non-hexagonal rings.[87,90] The STW defect is the 90° rotation of two carbon atoms connected by short-ranged covalent bond with respect to the midpoint of the bond. As illustrated in Figure 8, transformation of four adjacent hexagonal unit cells into two pentagonal and two heptagonal unit cells,[90] due to 2 pentagons and 2 heptagons transformations STW defects, are also known as 5-7-7-5 defects.

In addition to the above-mentioned classification, STW defects can also be sub classified according to their orientation in the graphene. As illustrated in Figure 8, pentagons can be separated by heptagons either horizontally (Figure 8a) or at an angle (Figure 8b), the former and later are known as STW1 and

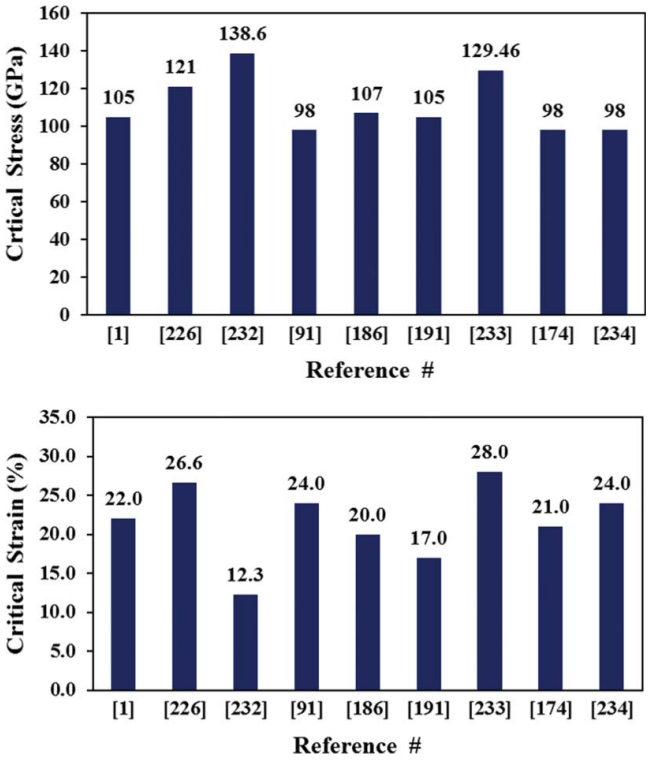

FIG. 7. Critcal stress and strain of pristine graphene in Zig-zag direction. Molecular Dynamics - [1, 91, 174, 186,191,234], Quantum Mechanics - [226,232], and Structural Mechanics [233].

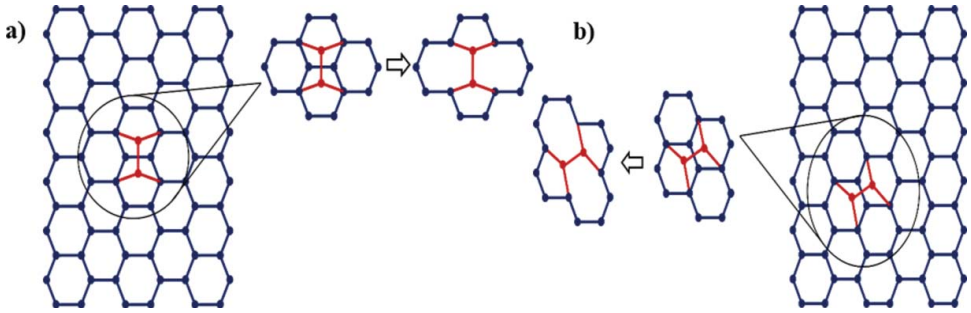

FIG. 8. Formation of Stone-Thrower-Wales defects (a) STW1 defects and (b) STW2.

STW2 defects, respectively.[1] During the last couple of years, researchers are extensively studying the effect of these defects on the mechanical and fracture properties of graphene. In 2013, Robertson and his team reported the recent advances in atomic resolution imaging of graphene. They used the aberration corrected high resolution transmission electron microscopy for inferring the deviation in the structure of pristine graphene due to defects such as vacancy, STW, impurities etc.[90]

The most significant contribution in this field has been made by using numerical-based approaches. Ansari et al.[14] used molecular dynamics based approach to study the impact of STW defects on the Young's modulus of graphene. Those simulations were performed with Tersoff-Brenner potential and Nose-Hoover thermostat for managing the interatomic interactions and temperature of the simulation box, respectively. From their research work, it can be inferred that failure strain and intrinsic strength of single graphene sheet is significantly reduced, whereas Young's modulus is slightly affected in presence of defects such as STW and vacancy. In addition to that, lower impact of defects in the armchair direction has been reported in the same research work.[14]

Xia et al.[216] proposed a finite element-based atomistic model for characterizing the elastic constants of graphene sheet with or without defects. In their proposed finite element model, commonly used modified Morse potential has been employed for simulating the atomic interaction between the atoms. They also introduced the interaction approach for modeling the formation of STW defects in carbon based nanofillers. In 2013, Bohayra et al.[250] investigated the impact of defect concentration on the mechanical properties of graphene. STW and di-vacancy defects were considered during the modeling, and it was reported in their article that with the increase in defects the elastic modulus of graphene decreases gradually. Di-vacancy defects were reported to have more impact on the elastic modulus of graphene as compared to STW defects. Similar trends were reported in the Hao et al.,[251] where it was concluded that concentration of STW defects have mild impact on the Young's modulus as compared to thermal conductivity of the graphene.

The mechanical properties of graphene are influenced by different possible prompting factors (like number and types of STW defects, distance between two STW defects and position of STW defects), Wang et al.[252] studied the same by using molecular mechanics-based finite element method and they found that mechanical properties of grapheme with STW defects are dependent on chirality. Fan et al.[253] showed dependency of formation energy of STW defects with concentration of defects and applied strain direction; this indicates anisotropic behavior of strain energy under high strain, so one can use graphene for strain-based devices. Rodrigues et al.[177] studied the effect of STW defects on edge reconstruction of zigzag graphene by first principle calculations and recently Dewapriya et al.[152] simulated the influence of free edges on the mechanical properties of graphene by using molecular dynamics.

In Baimova et al.,[5] once again the molecular dynamics-based approach was employed for simulating the impact of STW in conjunction with edge and temperature effects on the single sheet of graphene. Simulations were reported to be performed at zero and finite temperatures to estimate the activation energy of fracture in graphene. It was concluded in the same article that hydrostatic pressure and tension has significant effect on the mechanical properties of arm-chair graphene in presence of STW defects, whereas no impact was reported for the same defects in zig-zag configuration of graphene. He et al.[196] employed the molecular dynamics-based approach for simulating the effect of STW tilting angle (STW1 and STW2) on the mechanical properties of graphene. They reported that with STW1 defective graphene, the strength of arm chair configuration is much lower than the zig-zag, whereas the opposite trend was reported with STW2 defects.

Some of the researchers have also attempted to model the effect of STW defect on the fracture strength of single graphene sheet.[1,14,216] Wang et al.[1] employed the molecular dynamics based atomistic simulations for investigating the fracture strength of graphene in presence of STW and vacancy defects. It was reported in their research work that defects such as STW significantly reduced the fracture strength of graphene. Their research work also helps in concluding that simulations performed at increased temperature and strain favors the formation of STW defects via bond rotation. It can be

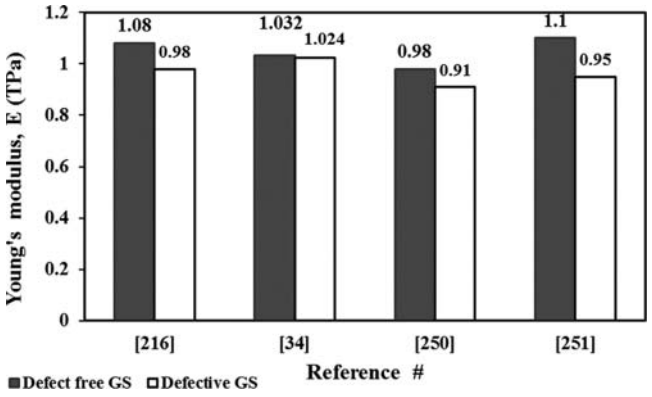

FIG. 9. Spectrum of Young's modulus value with pristine graphene sheet and STW defected graphene. Finite Element Method – [216] and, Molecular Dynamics [34, 250, 251].

inferred from Xiao et al.[216] that STW defects significantly reduce the failure strain, ultimate strength of nanofillers. Authors made an attempt in Figure 9 to compile the effect of STW defects on the Young's modulus of graphene studied by various researchers.

Zacharias and his research team performed molecular dynamics-based simulations to study the effect of temperature and STW defects on the thermal conductivity of a single graphene sheet.[254] It was concluded in their simulation results that increase in STW defects and temperature has a negative impact on the thermal conductivity of the graphene. In a similar study, it was established that the variation of thermal conductivity with changes in temperature is less significant in the presence of larger number of STW defects.[255] Moreover, in the same research work[255] the thermal conductivity in armchair direction was reported lower than the zigzag direction regardless to the number of defects. Yang et al.[249] also employed a molecular dynamics-based simulation to study the STW defects and their orientation on the thermal conductivity of the graphene. It was reported in the research work[249] that arrays of STW defects perpendicular to the direction of heat flow can be regarded as grain boundaries, which might act as a barrier to the phonon transmission and limit the mean free path.[249]

3.2.2. *Vacancy Defects*

The absence of atoms from the lattice of graphene is usually termed as vacancy defects, which can be further sub classified as mono-vacancy, di-vacancy, and multi-vacancy defects based on number of atoms absent from the lattice of graphene. The absence of single carbon atom from the graphene lattice yields a mono-vacancy, which left the graphene lattice with three under coordinated edge carbon atoms, each of them possesses a single dangling bond;[90] an atomistic model of pristine graphene is shown in Figure 10a. Removal of the highlighted carbon atom in Figure 10a, forming mono vacancy with metastable configuration which can undergo Jhan-Teller distortion[90,256] and reconstructing the pattern, os shown in Figure 10c.

The di-vacancy can be created by the removal of two carbon atoms from the pristine graphene or coalescence of two mono vacancies, as demonstrated in Figures 11a–c. It can be inferred from Figure 10c (mono-vacancy) and Figure 11c (di-vacancy) that one can expect under coordinated carbon atoms in mono vacancy, whereas the di-vacancy does not have any under coordinated carbon atoms after reconstruction, it can be concluded from this sub section that di-vacancy are more stable under irradiation as all of the carbon atoms are sp^2 bonded.[34,90]

In general, graphene sheet can have chances of forming STW defects in addition to di-vacancy and can form different configurations.[257–259] The bond highlighted in red in the atomistic model of 5-8-5 (Figure 11c) configuration can go through a STW rotation and yielding 555-777 structure as shown in atomistic model of 555-777 (Figure 11d) configurations. The bond highlighted in red (Figure 11e) can also go through STW rotation and forming 5555-6-7777 structure, as shown in atomistic model of 5555-6-7777 (Figure 11f).

The removal of more than two carbon atoms can lead to a multi-vacancy defect which is larger and have a more complex defect configuration as illustrated in Figures 12a and 12b. An

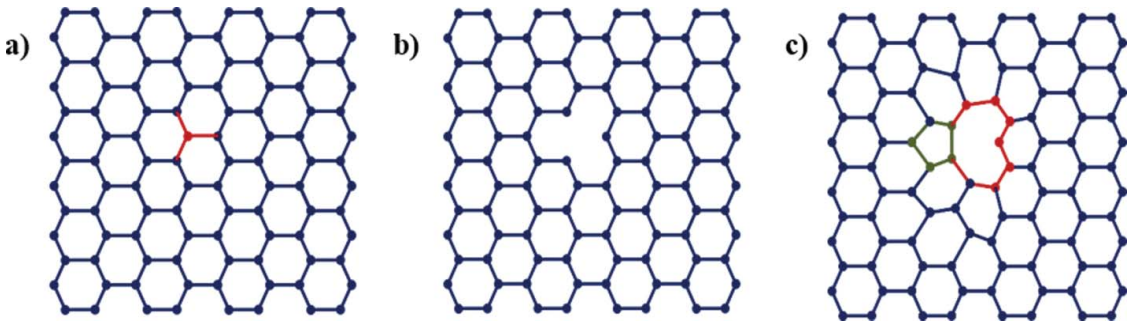

FIG. 10. (a) Atomistic model of a graphene sheet, (b) removal of C-atom highlighted in (a) forming mono-vacancy with metastable configuration (three dangling bond), and (c) reconstruction of graphene lattice after Jahn-Teller distortion due to metastable configuration.

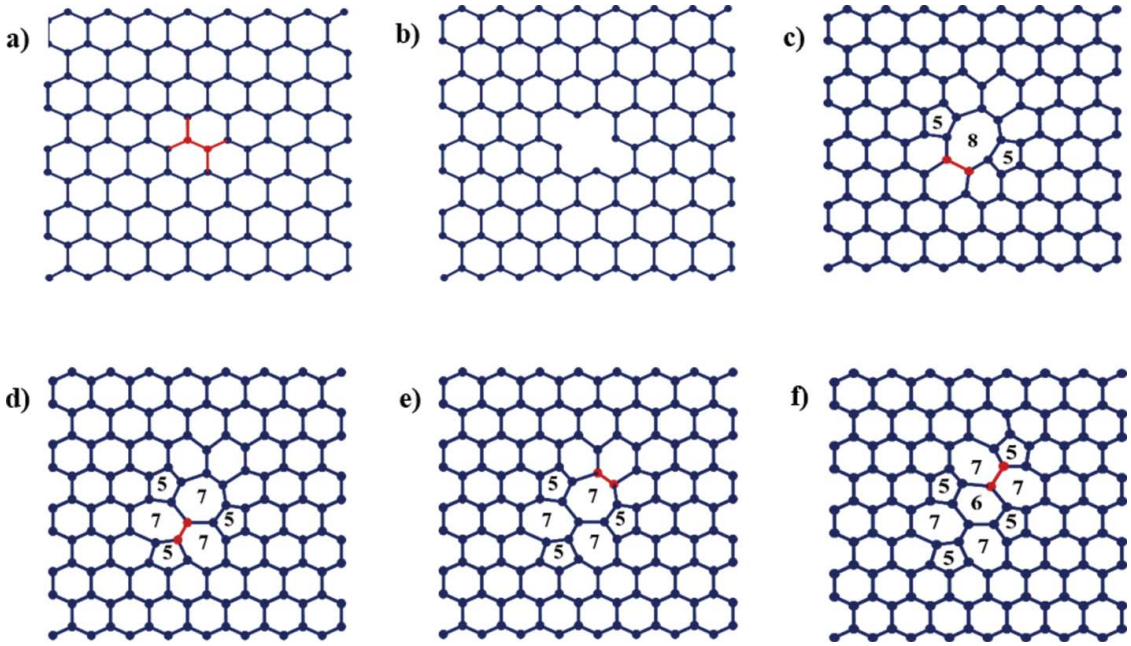

FIG. 11. (a) Atomistic model of pristine graphene; (b) removal of C-atoms highlighted in (a) forming DV with four dangling bonds; (c) atomistic model of reconstructed structure of graphene sheet with DV into stable 5-8-5 configuration; (d) SW rotation of highlighted atoms in (c) forming 555-777 structure; (e) atomistic model of 555-777 configuration; and (f) SW rotation of highlighted atoms in (e) forming 5555-6-7777 structure.

even number of missing atoms from the graphene lattice usually leads to a complete reconstruction, whereas an odd number of vacancy defects no such reconstruction is possible. Due to this reason, even numbers of vacancies are energetically favored structures. The same conclusion has been made in Jing et al.[34] that Young's modulus of graphene with mono vacancy defects is lower as compared to di-vacancy defects with the same number of missing atoms.

Effect of these vacancy defected graphene lattice was investigated by many researchers.[34,86,181,214,251,256,260–262] As reported earlier, Robertson et al.[90] employed the aberration corrected electron transmission microscopy to investigate the effect of vacancy on the mechanical properties of graphene. In addition to this experimental work, one pioneering research was published in 2004 discussing the characterization of defective graphene sheets with the help of transmission electron microscope (TEM).[263]

Zandiatashbar et al.[2] discussed the effect of defects on the mechanical properties of graphene. It was reported in their experimental work[2] that elastic modulus of graphene sheet is maintained even at a high density of sp3 type defects, whereas the overall 14% reduction in the fracture strength was observed for a defective graphene as compared to pristine graphene. On the other hand, a significant reduction in the mechanical properties was reported in the same paper with vacancy defects.[2] Zandiatashbar et al.[2] also provided a trend between the Raman spectra of defective graphene and its mechanical properties, which helps in identifying the defective graphene sheets that are still functional. Jian et al.[86] proposed a molecular dynamics-based atomistic model to study the effect of different vacancy configurations (e.g., rectangular and circular), size and concentration of these vacancy defects on the Young's modulus of the graphene sheet as referred in Figures 12c and 12d. The atomistic model[86] helps in concluding that vacancies aligned in the direction perpendicular to the loading direction has more impact on the Young's modulus of the defective graphene. In addition to that a linear reduction in the Young's modulus was observed with the increasing concentration of mono atomic vacancy defects.[86] The same atomistic model was further extended to study the effect of these defects on the fracture strength, crack initiation, and propagation.[86] Blunting of vacancy edges was reported in Jian et al.[86] and fracture behavior of defective graphene was reported to be the function of shape of the vacancy in the lattice of graphene as illustrated in Figures 12c and 12d. When a material contains multiple defects, it is expected that the stress concentration of these defects superposes if the separation distances of the defects are low, which causes a more reduction in the strength.

Yadav et al.[94] used DFT calculations to study the significance of van der Waals forces on hydrogen molecule absorption. They studied the effect of point defects on hydrogen binding ability of graphene. Sharma et al.[172] also performed molecular dynamics based simulations to study the effect of point defects on the mechanical properties of CNT. Effect of graphene with pinhole defects (Figure 12d) were explored by

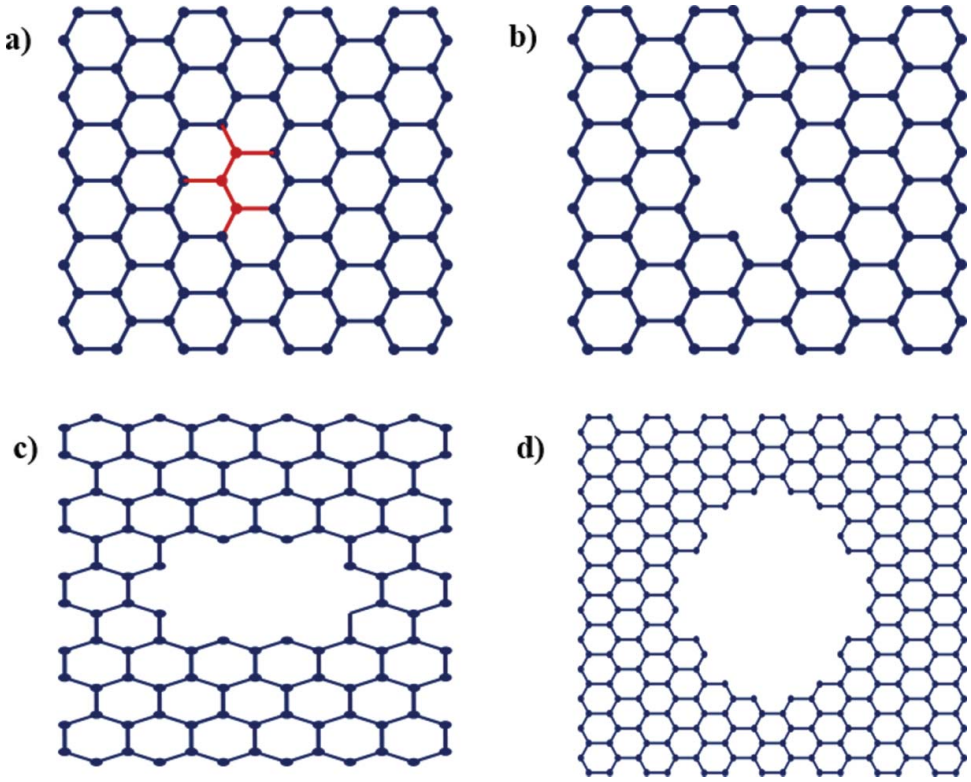

FIG. 12. (a) Atomistic model of pristine graphene; (b) removal of C-atoms highlighted in (a) forming multi vacancy defects; and (c) and (d) Rectangular profile and Circular profile (pinhole) of multi-vacancy defects, respectively.

Georgantzinos et al.[233] using structural mechanics approach (nonlinear) and examined the impact of hole size on elastic and failure-related properties.

Jing and his research team[34] also used molecular dynamics-based simulations to study the effect of STW and vacancy on the Young's modulus of graphene. Atomistic modeling performed by their team helps in concluding the reduction in Young's modulus with the increase in concentration and degree of defects. Reconstruction in vacancy-induced graphene sheets usually helps in stabilizing the Young's modulus. The same atomistic model proposed in Jiang et al.[34] further extended to study the effect of hydrogenated defects on the Young's modulus of the graphene. It was reported in the results that hydrogenation of vacancy defects have positive impact whereas STW defects have negative impact on the Young's modulus of the defective graphene. The trend and results reported in this Jiang et al.[34] agreed with the results presented in Mortazavi and Ahzi.[250] Yang et al.[264] also used the molecular dynamics-based approach for characterizing the effect of randomly distributed vacancy defects on the mechanical properties of graphene sheet. Recently, Tapia et al.[219] proposed the finite element-based atomistic model to study the effect of distribution and concentration of vacancy defects of the elastic constants of graphene sheet. It was reported in Tapia et al.[219] that position of these vacancy defects has significant impact on the shear modulus and Poisson's ratio of graphene. Finite element-based atomistic model was used by Canadija et al.[218] to study the effect of vacancy location and concentration on the bending behavior of graphene. It was concluded from the finite element model that vacancy defects lying in the center of graphene has more influence on the bending strength of graphene. Importance of location of vacancy defects are also examined by Santana et al.[265] by using DFT calculations, mono-vacancy defects in graphene near the edges are energetically favor than the same in the middle of the graphene sheet. In Figure 13, the authors made an attempt to compile the effect of vacancy defects on the Young's modulus of graphene studied by various researchers.

Authors also made an attempt to plot the average change in Young's modulus of graphene due to STW and vacancy defects Figure 14. The results plotted in Figures 9 and 13 with respect to STW and vacancy defects is averaged and compiled in Figure 14. It can be concluded with the help of Figure 14 that vacancy defects are more detrimental to the Young's modulus of single sheet of graphene as compared to STW defects.

On the other hand, it is believed that if the locations of defects are distinct enough such that their affected areas are distinct, their behavior is similar to a material with single defect.[183] Finite element based atomistic model had been proposed by Baykasoglu et al.[124] to study the effect of STW and single vacancy on the arm chair and zig zag configuration of defective graphene. Large deformation and nonlinear properties were considered for

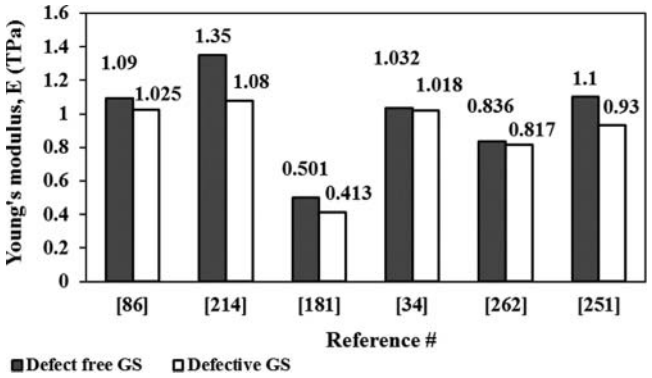

FIG. 13. Spectrum of Young's modulus with pristine graphene and vacancy defected graphene. Molecular Dynamics - [34, 86, 181, 214, 251, 262].

simulating the bonded atoms of graphene with the help of modified Morse potential. It was concluded in Baykasoglu et al.[124] that large deformation and nonlinear geometric effects are important on the fracture behavior of graphene sheets. The results show that graphene sheets exhibits an orthotropic fracture behavior and these defects significantly affect the mechanical performance of the graphene sheets.[124]

The contribution of various researchers to investigate the effect of STW and vacancy defects on mechanical properties of graphene is compiled and tabulated in Table 2.

It was reported in the Mortazavi and Ahzi[250] that even a 0.27% concentration of vacancy can reduce the thermal conductivity by 50%. Thermal conductivity of defective graphene sheet reduces at a rapid rate at small density (0.2%) of defects, but reduction becomes gradual at higher concentration of defects.[267] The same trend was reported in the research work of Hao et al.[268] and Sevik et al.[269]

Zhang and his team performed molecular dynamics-based simulations to compare the effect of single vacancy (SV), divacancy (DV), and STW defects on the thermal conductivity

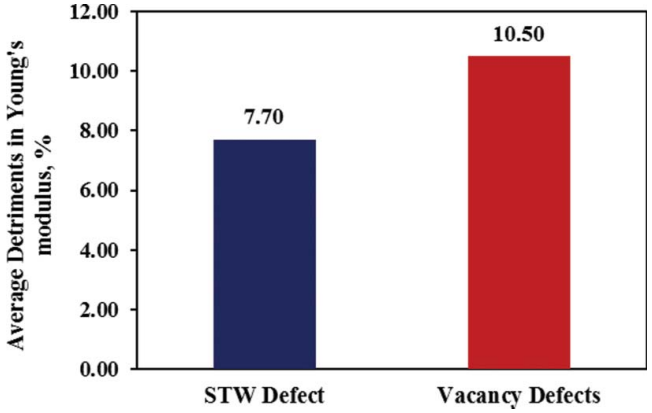

FIG. 14. Average decrease in Young's modulus with STW defect and vacancy defect of graphene sheet.

of graphene.[267] They used defect density (defined as the number of defects divided by the number of atoms in the pristine graphene), where each defect is treated as an individual scattering center, independent of the defect type or the number of atoms that forms it.[269]

At small defect density (i.e., 0.2%), the SV-defective graphene possesses the highest thermal conductivity, followed by DV and STW graphene. In other words, the presence of small amount of SV leads to the smallest reduction in thermal conductivity. Based on the present defect density definition, at the same defect density, all the defective graphene have the same number of defective centers. However, in each defective center, one atom is missing in the SV-defective graphene while two atoms are missing in DV-defective graphene. The total missing atoms in SV-graphene are half of those in DV-graphene. Therefore, more phonon–defect scattering is stimulated in DV-graphene and consequently it undergoes more severe deterioration in thermal conductivity than its SV-counterpart.[267]

In contrast to the findings of Zhang et al.[267] are the results published by Haskins et al.[270] In their research,[270] it was concluded that SVs are more efficient in decreasing thermal conductivity of graphene nano-ribbons (GNRs) compared to DV and STW at the same defect density because of their less stable two coordinated atoms. In the work of Haskins et al.,[270] the defect density is defined as the number of defected atoms divided by the total atom number in pristine graphene. The revised values are close to each other, indicating that SV and DV at the relative high density level have the same effect on thermal conductivity. When the defect density is larger than 0.5%, the thermal conductivity of the graphene with three different defects is rather close to each other with minor difference.[267] With increasing defect concentration, the reduction in thermal conductivity is dominated by the defect density rather than the defect types. All the defective graphene with different types of defects possess close thermal conductivity at the same defect density.[267] Pang et al.[271] used MD based simulations to investigate the effect of triangular vacancy defects on the thermal transport property of armchair graphene nano-ribbons. Two important observations were reported in the same paper: first, thermal conductivity of graphene nano-ribbons decreases with increase in the size of defect; and second, the thermal conductivity of these nano-ribbons becomes insensitive to temperature range at higher concentration of defects.[271] Liu and his team of researchers studied the effect of defect location on the thermal conductivity of graphene nano-ribbons.[272] Molecular dynamics-based atomistic models were developed in their numerical investigations to study the effect of horizontally or vertically aligned defects with respect to the direction of heat flow. It was also reported in their work that thermal conductivity of graphene nano-ribbons gradually decreases on moving the defects from the edge to the middle of the graphene nano-ribbons. Authors have made an attempt to compile the research work of different scientists in the area of fracture strength of graphene sheet and these are presented in Table 3.

TABLE 2
Young's modulus of pristine and defective graphene found by different researchers

Studied by	Conditions / Types of Defects	Methods Adopted	Young's Modulus (TPa)	Poisson's Ratio
Jiang et al.[179]	T = 100–500 K	Molecular Dynamics	0.95 – 1.1	0.17
Shen et al.[210]	T = 300–700 K	Molecular Dynamics	0.905	
Lee et al.[208]	Pristine graphene	Experiment	1 ± 0.1	
Tsai et al.[180]	NPT ensemble	Molecular Dynamics	0.912	0.261
	NVT ensemble		0.912	0.26
Kvashnin et al.[214]	Vacancy defects	Molecular Mechanics	1.08	
Neek-Amal et al.[181]	0% vacancy defects	Molecular Dynamics	0.501 ± 0.032	
	randomly distributed vacancy defects		0.413 ± 0.019	
Ni et al.[182]	Pristine graphene	Molecular Dynamics	1.09 (average)	
Reddy et al.[213]	With mini of PE of graphene	Continuum Mechanics	0.669	0.416
	Without mini of PE of graphene		1.012	0.245
Liu et al.[226]	Pristine graphene	Density Functional Theory	1.05	
Shokrieh et al.[215]	Pristine graphene	Continuum Mechanics	1.04	
Yanovsky et al.[232]	Pristine graphene	Quantum Mechanics	0.737	
Xiao et al.[216]	Stone -Wales defect	Finite Element Method	0.98	
Georgantzinos et al.[217]	Pristine graphene	Finite Element Method	1.367	
Sakhaee-Pour [123]	Pristine graphene	Finite Element Method	1.025	
Jani Kotakoski et al.[266]	Grain Boundaries	Molecular Dynamics	0.6	
Zhu Jian et al.[86]	Vacancy	Molecular Dynamics	1.090 ± 0.003	0.2
R.Ansary et al.[183]	Double Vacancy	Molecular Dynamics	0.7985	
Zhang et al.[184]	T = 300–2000 K	Molecular Dynamics	1.11 – 0.847	
	Isotope substitutions		1.085 (average)	
R.Ansary et al.[14]	STW defects	Molecular Dynamics	60% reduction	
Nuannuan Jing et al.[34]	Vacancy defects	Molecular Dynamics	1.0186	
	STW defects		1.0244	
Akihiko Ito[262]	Vacancy defects	Molecular Dynamics	0.817	
Zhang et al.[199]	Pristine graphene	Experiment	0.89	
Daniel et al.[227]	Pristine graphene	Density Functional Theory	1.07	0.14–0.19
Hernandez et al.[228]	Pristine graphene	Tight Binding	1.206	
Gupta et al.[222]	Pristine graphene	Molecular Dynamics	1.272	0.147
WenXing et al.[223]	Pristine graphene	Molecular Dynamics	1.026	
Meo et al.[229]	Pristine graphene	Finite Element Method	0.945	
Pei et al.[191]	Hydrogen functionalized graphene	Molecular Dynamics	0.86	
Hemmasizadeh et al.[224]	Pristine graphene	Molecular Dynamics / Continuum Mechanics	0.939	
Neek-Amal et al.[225]	Pristine bi-layer graphene	Molecular Dynamics / Experiment	0.8	
Feng Hao et al.[251]	STW	Molecular Dynamics	0.95	
	Vacancy	Molecular Dynamics	0.93	

3.2.3. Dislocations and Grain Boundaries

In general, vacancy and STW are considered as common defects in graphene and are extensively studied by many researchers.[14,34,86,123, 179–184,208,210,213–217,226,232,252,262,266,273] Limited research has been reported on class of defects such as dislocations and grain boundaries. Fracture toughness is known to be critically dependent on materials microstructures, and particularly on how dislocations are generated or multiplied at the crack tip.[230] This fundamental defect is of great interest to material scientists; it is a form of defects in which an extra half plane of atoms can deteriorate the strength of graphene.[274] Due to the two-dimensional (2D) nature of graphene, only edge dislocations

TABLE 3
Fracture Properties of defect free and defective graphene sheet found out by different researchers

Studied by	Types of Defects	Methods Adopted	Fracture Strength (GPa)	Fracture Strain
Zhu Jian et al.[86]	Vacancy defects	Molecular Dynamics	90.8	13.70%
R.Ansary etal.[183]	DV defects	Molecular Dynamics	108.8	18.41%
Yanovsky et al.[232]	Pristine graphene	Quantum Mechanics	90	12.30%
M.C.Wang et al.[1]	STW defects	Molecular Dynamics	88.479 (SW1) 61.8 (SW2)	
	Vacancy defects		62.7	
Xiao et al.[216]	STW defects	Finite Element Method	84.6 (average)	10%
Jani Kotakoski et al.[266]	Grain Boundaries	Molecular Dynamics	46	9%
Ni et al.[182]	Pristine graphene	Molecular Dynamics	195 (average)	38.17% (average)
Bu et al.[185]	Graphene Nanoribbons	Molecular Dynamics	175	30.26%
Lee et al.[208]	Pristine graphene	Experiment	130±10	25%
Pei et al.[191]	Pristine graphene	Molecular Dynamics	121	22%
Niaki et al.[231]	Pristine graphene	Molecular Dynamics	115	
Georgantzinos et al.[233]	Pristine graphene	Structural Mechanics	129.46	28%
Z. Xu [174]	Pristine graphene	Molecular Dynamics	98.00	21%
Liu et al.[226]	Pristine graphene	Density Functional Theory	110–121	19.4–26.6%
Ogata et al.[273]	Pristine graphene	Density Functional Theory	107	20.80%
Zhang et al.[184]	T = 300–2000 K	Molecular Dynamics	125.87 – 42.93	14.8% – 4.8%
	Isotope substitutions		129 (average)	17% (average)
Ansary et al.[14]	Vacancy defects	Molecular Dynamics	114.29 (average)	13.035% (average)
	STW defects		117.26 (average)	10.195% (average)

were studied by the researchers.[275] Complementary pair formed[82] due to the removal of zigzag chain of carbon atoms is shown in Figures 15a–c.

There are five different feasible mechanisms that illustrate how these dislocation pairs are formed in graphene sheet: (i) during the CVD growth, (ii) electron beam sputtering of carbon dimers, (iii) from surface adatom incorporation, (iv) from a mono-vacancy, and (v) from a STW defect.[276] Lee and his team[277] proposed an atomistic model based on tight binding molecular dynamics and ab-initio energy calculation to study the formation of dislocations from point defects in graphene. It was concluded in that article that the coalescence of 5–7 pairs with vacancy defects lead to the generation of dislocation in graphene. It was pointed out in the Lee et al.[277] that lower energy barrier favors the ejection of adatoms from graphene surface to form the dislocation in graphene lattice.

Butz et al.[278] reported one of the significant contributions on characterizing the dislocations in the bi-layer graphene sheets. In their research work both experimental as well as numerical techniques were employed to study the dislocations in graphene. Their observations were made with the help of transmission electron microscope (TEM). It was experimentally observed that in the absence of stacking fault energy, leads to dislocation pattern that corresponds to AB↔AC

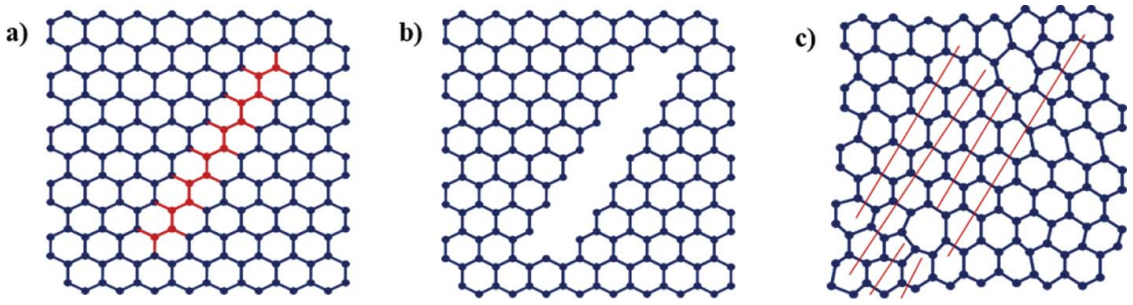

FIG. 15. (a) Atomistic model of single-layer graphene sheet; (b) the highlighted zigzag chain of atoms are removed; and (c) yield a dislocation pair with two pentagon-heptagon cores.

stacking order in graphene. Ab-initio based numerical approach was reported in Yazyev and Louie[275] to investigate the thermodynamic and electronic properties of the topological defects such as dislocations and grain boundaries. It can be inferred from this review that numerical-based approach such as molecular dynamics; tight binding molecular dynamics are extensity used by the researchers to study the defects in graphene. One more molecular dynamics-based study was reported in Ariza et al.[279] to study the dynamic stability of dislocations in graphene lattice. Two conclusions have been made after simulating dislocations in graphene. The first of these dislocations are dynamically stable up to the temperature of 2500 K and with the second, discrete dislocation theory is capable of predicting the energies of these kind of systems. Carpio et al.[280] also studied the evolution and stability of defects such as dislocations in single sheet of graphene. Bonilla et al.[274] reported in a letter that movement of dislocation is an important parameter that determines the strength of graphene.

Grain boundaries by definition are line defects (composed of dislocation), separating graphene grains (domains/crystallites) with different crystal lattice orientations. More accurately, each grain boundaries in a 2D graphene separates two grains whose crystal lattices are rotated/tilted relative to each other by a tilt mis-orientation angle θ, with the rotation axis being perpendicular to the sheet plane.[266]

Even though mechanical exfoliation using "scotch-tape" method shows exceptional properties,[86] still it is not suitable for large-scale instrument fabrication. Since the chemical vapor deposition (CVD) is currently the only way for producing industry-scale graphene membranes and it leads to polycrystalline samples. This can significantly influence the properties of a two-dimensional material and study of grain boundary in graphene has become of fundamental importance.[266]

It can be inferred from the above sections that extensive efforts has been made by the researchers to study the vacancy and STW defects in graphene but, limited efforts has been made by research community to study dislocations and grain boundaries in graphene. Even the first experimental-[266] based study on polycrystalline graphene was carried out in 2011. Nemes-Incze et al.[281] proposed selective oxidation of defects and then atomic force microscope analysis to study the polycrystalline nature of graphene. It was claimed in Nemes-Incze et al.[281] that proposed AFM technique is quick and easy for quantifying the quality of graphene produced by chemical vapor deposition. Rasool et al.[282] employed transmission electron microscope for characterizing the single and bi-crystals of graphene that were synthesizes by CVD technique. Subsequently, atomic force microscope (AFM) was used to estimate the mechanical properties of these graphene crystals. Mechanical properties of graphene synthesized by CVD are largely dominated by grain boundary, and at least mis-orientation of grains and rotation of grain boundary line is required for characterizing the effect of these grain boundary on the properties of graphene. The same degrees of freedom, mis-orientation, and rotation of grain boundary line was also pronounced as important factors for characterizing the mechanical properties of graphene in Wu and Wei.[197] Recently, Xu et al.[283] used scanning tunneling microscopy to identify line defects by experimentally. In 2012, Jhon et al.[198] used the molecular dynamics based approach to study the effect of tilted and non-tilted grain boundaries on graphene. In that numerical study, simulations were performed with tensile as well as compressive loading aligned parallel or perpendicular to the grain boundaries. As compared to the fracture behavior of pristine, and graphene with non-tilted grain boundaries, the graphene with tilted grain boundary had shown a distinctive response to tensile loading applied perpendicular to the grain boundary. Atomic force microscopy was once again used by the authors of Ruiz-Vargas et al.[284] for imaging grain boundary and ripples in the single sheet of graphene. It was observed in Ruiz-Vargas et al.[284] that grain boundaries significantly reduced the breaking strength of graphene. Molecular dynamics-based simulations were also reported in the same article to conclude that grain boundaries are more detrimental to the strength of graphene in the presence of voids. Kotakoski et al.[266] showed that the presence of grain boundaries reduces the strength of graphene by approximately 50% (down to ~46 GPa), and the results were also validated with the help of experiments. It can be inferred from the discussions that mis-orientation angles of grain boundary are important for the properties of the poly crystalline material. Keeping this in mind, Liu et al.[285] employed the molecular dynamics based approach to study the range of mis-orientation for the bi-crystals of graphene. Range of mis-orientation starting from 0–60° was considered in that numerical simulation.

From these discussions, one can easily infer that polycrystalline graphene is the only possible solution to achieve industrial-scale large graphene sheets. Grain boundaries have complicated impact on the properties of graphene sheet, as large angle tilt boundaries (which have a high density of defects) may be much stronger than that with low angle boundaries.[286] Yi et al.[286] investigated the effects of temperature and strain rate on the strength of mono layer of graphene. It was reported in the paper that a graphene sheet with tilt grain boundaries are more affected by the defects as compared to pristine form of graphene. Grain boundaries have detrimental effect on the strength of graphene sheets at higher temperatures.

In 2015, Chen et al.[287] investigated the effects of grain size, temperature, and strain rate on the mechanical properties of polycrystalline graphene by using MD simulations. Mechanical properties like Young's modulus and fracture strength are considered as sensitive to grain size, temperature and strain rate. Yin et al.[288] investigated the effect of line defects on single-layer graphene sheets by MD based simulation. In their simulations, impact of location of defects, number of defects has been studied to regulate the

graphene structure. In one more recent publication of 2015, Zhang et al.[89] used MD-based simulations to demonstrate the toughness of graphene. A nodel design technique as a combination of field crystal method and atomistic simulations has been proposed in Zhang et al.[89] to solve the inverse problem of finding the optimized defect distribution and type of topological defects that make a graphene sheet conform to a targeted 3D surface.

Hao et al.[289] constructed polycrystalline graphene sheet with tilt grain boundaries and studied the mechanics of the same using molecular dynamics simulation. Local buckling in the form of ridges and funnels were reported in the simulations due to high compressive stress states in pentagons. Zhang et al.[290] studied mechanical properties of 20 representative grain boundaries in graphene using molecular dynamics and density functional theory. It was reported in this article that the grain boundary may remain flat or become inflected up to 72°C with different arrangements of heptagon and pentagon rings which is formed by Stone-Wales transformation. SW transformation is the major failure mechanism of graphene grain boundary at high temperatures but the initial fracture site can be on the boundary line or inside the domain. Kim et al.[243] carried out experimental and theoretical studies on cracks or tears in monolayer graphene.

4. FEATURE ASPECTS

This article reveals that a comprehensive understanding of strong structure-property relations is necessary for development of novel graphene-based materials and graphene-based nanocomposites for engineering applications. However, there still exists some knowledge gaps in this area; more research is indeed required to be performed to clarify the underlying deformation mechanisms of the strong structure-property relations for further improvement. Like any other real engineering material, atomistic defects do exist in graphene and can drastically alter its mechanical and fracture properties. So for, extensive research work has been done to find out structural-property relations by considering some popular defects in mono-crystalline graphene, such as Stone-Thrower-Wales (STW) defect and Vacancy (Mono-vacancy and di-vacancy) defects. However, due to increasing demand of graphene, it is necessary to produce graphene in large scale by the CVD exfoliation method. This leads to polycrystalline graphene and some other atomistic defects such as dislocation, grain boundaries, adatoms, and interstitials that can be formed due to a polycrystalline nature and have to be analyzed under various boundary conditions.

5. SUMMARY

This article on the effect of defects on the mechanical properties, thermal conductivity, and fracture behavior of graphene was carried out to study structural-property relation.

The following value-adding points were derived from this comprehensive article.

- Both Stone-Wales (S-W) and vacancy defects can deteriorate the strength and thermal conductivity of graphene, but the impact of vacancy defects is more significant as compared to STW defects due to higher number of dangling bonds.
- Formation of STW defects via bond rotation in graphene is reported to be a function of temperature, loading level, and loading direction.
- It can be inferred that Young's modulus of graphene is a function of type, location, degree, orientation, and size of defects. For example, it has been reported that the critical strength and strain of pristine graphene in armchair direction is higher than zig-zag direction.
- It can be concluded that the fracture strength of graphene depends on a number of vacancy defects, distance between the vacancy defects, and temperature.
- There is more evidence to be found that mechanical and fracture properties of graphene with grain boundaries mainly depend on tilt angle of grain boundaries and temperature.
- It can be inferred that strength of graphene also depends on the potential employed for simulating the interatomic interactions as well as range of cutoff radius used in the simulations.

REFERENCES

1. M. C. Wang, C. Yan, L. Ma, N. Hu, and M. W. Chen, Effect of defects on fracture strength of graphene sheets, *Comput. Mater. Sci.* **54**, 236–239 (2012).
2. A. Zandiatashbar, G. H. Lee, S. J. An, S. Lee, N. Mathew, M. Terroness, T. Hayashi, C. R. Picu, J. Hone, and N. Koratkar, Effect of defects on the intrinsic strength and stiffness of graphene, *Nat. Commun.* **5**, 3186 (2014).
3. M. C. Wang, C. Yan, D. Galpaya, B. L. Zheng, L. Ma, N. Hu, Q. Yuan, R. Bai, and L. Zhou, Molecular dynamics simulation of fracture strength and morphology of defective graphene, *J. Nano Res.* **23**, 43–49 (2013).
4. A. A. Balandin, S. Ghosh, W. Bao, I. Calizo, D. Teweldebrhan, M. Feng, and C. N. Lau, Superior thermal conductivity of single-layer graphene, *Nano Lett.* **8**, 902 (2008).
5. J. A. Baimova, L. Bo, S. V. Dmitriev, K. Zhou, and A. A. Nazarov, Effect of Stone-Thrower-Wales defect on structural stability of graphene at zero and finite temperature, *EPL* **103**, 46001 (2013).
6. L. Xiao, H. M. Thomas, J. T. Robinson, B. H. Houston, and F. Scarpa, Shear modulus of monolayer graphene prepared by chemical vapor deposition, *Nano Lett.* **12**, 1013–1017 (2012).
7. R. Gillen, M. Mohr, and J. Maultzsch, Raman-active modes in graphene nanoribbons, *Phys. Status Solidi B* **247**, 2941–2944 (2010).

8. A. Bosak, M. Krisch, M. Mohr, J. Maultzsch, and C. Thomsen, Elasticity of single-crystalline graphite: Inelastic x-ray scattering study, *Phys. Rev. B Condens. Matter* **75**, 153408 (2007).
9. S. V. Dmitrriev, J. A. Baimoya, A. V. Savin, and Y. S. Kivshar, Ultimate strength, ripples, sound velocities, and density of phonon states of strained graphene, *Comput. Mater. Sci.* **53**, 194–203 (2012).
10. K. V. Zakharchenko, J. H. Los, M. I. Katsnelson, and A. Fasolino, Atomistic simulations of structural and thermodynamic properties of bilayer graphene, *Phys. Rev. B Condens. Matter* **81**, 235439 (1–6) (2010).
11. Y. Zhu, S. Murali, W. Cai, X. Li, J. W. Suk, J. R. Potts, and R. S. Ruoff, Graphene and graphene oxide: synthesis, properties, and applications, *Adv. Mater.* **22**, 3906–3924 (2010).
12. R. S. Edwards and K. S. Coleman, Graphene synthesis: relationship to applications, *Nanoscale* **5**, 38–51 (2013).
13. K. I. Bolotin, K. J. Sikes, Z. Jiang, M. Klima, G. Fudenberg, J. Hone, P. Kim, and H. L. Stormer, Ultrahigh electron mobility in suspended graphene, *Solid State Commun.* **146**, 351–355 (2008).
14. R. Ansari, S. Ajori, and B. Motevalli, Mechanical properties of defective single-layered graphene sheets via molecular dynamics simulation, *Superlattices Microstruct.* **51**, 274–289 (2012).
15. A. M. Fennimore, T. D. Yuzvinsky, W. Q. Han, M. S. Fuhrer, J. Cumings, and A. Zettl, Rotational actuators based on nanotubes, *Nature* **424** (24), 408–410 (2003).
16. B. L. Allen, P. D. Kichambare, and A. Star, Carbon nanotube field-effect-transistor-based biosensors, *Adv. Mater.* **19**, 1439–1451 (2007).
17. J. Cumings and A. Zettl, Low-friction nanoscale linear bearing realized from multiwall carbon nanotubes, *Science* **289**, 602–604 (2000).
18. A. Bianco, K. Kostarelos, and M. Prato, Applications of carbon nanotubes in drug delivery, *Curr. Opin. Chem. Biol.* **9**, 674–679 (2005).
19. M. R. Banwaskar and S. N. Dachawar, Graphene basics and applications, *Adv. Mater. Res.* **622–623**, 259–262 (2013).
20. P. Avouris and C. Dimitrakopoulos, Graphene: synthesis and applications, *Mater. Today* **15**, 86–97 (2012).
21. X. Huang, Z. Yin, S. Wu, X. Qi, Q. He, Q. Zhang, Q. Yan, F. Boey, and H. Zhang, Graphene-based materials: synthesis, characterization, properties, and applications, *Nano Micro Small* **7** (14), 1876–1902 (2011).
22. A. Sakhaee-pour, M. T. Ahmadian, and A. Vafai, Potential application of single-layered graphene sheet as strain sensor, *Solid State Commun.* **147**, 336–340 (2008).
23. W. Choi, I. Lahiri, R. Seelaboyina, and Y. S Kang, Synthesis of graphene and its applications: a review, *Crit. Rev. Solid State Mater. Sci.* **35**:1, 52–71 (2010).
24. T. Kuila, S. Bose, P. Khanra, A. K. Mishra, N. H. Kim, and J. H. Lee, Recent advances in graphene-based biosensors, *Biosens. Bioelectron*. **26**, 4637–4648 (2011).
25. M. S. Artiles, C. S. Rout, and T. S. Fisher, Graphene-based hybrid materials and devices for biosensing, *Adv. Drug Delivery Rev.* **63**, 1352–1360 (2011).
26. M. Pumera, Graphene in biosensing, *Mater. Today* **14**, 308–315 (2011).
27. S. Ebrahimi, A. Montazeri, and H. Rafii-Tabar, Molecular dynamics study of the interfacial mechanical properties of the graphene-collagen biological nanocomposite, *Comput. Mater. Sci.* **69**, 29–39 (2013).
28. Y. Sun, Q. Wu, and G. Shi, Graphene based new energy materials, *Energy Environ. Sci.* **4**, 1113–1132 (2011).
29. M. Pumera, Graphene-based nanomaterials for energy storage, *Energy Environ. Sci.* **4**, 668–674 (2011).
30. D. A. C. Brownson, D. K. Kampouris, and C. E. Banks, An overview of graphene in energy production and storage applications, *J. Power Sour.* **196**, 4873–4885 (2011).
31. Q. Huang, D. Zeng, S. Tian, and C. Xie, Synthesis of defect graphene and its application for room temperature humidity sensing, *Mater. Lett.* **83**, 76–79 (2012).
32. D. Berman, A. Erdemir, and A. V. Sumant, Graphene: a new emerging lubricant, *Mater. Today* **17**(1), 31–42 (2014).
33. G. D. Zhan, J. D. Kuntz, J. Wan, and A. K. Mukherjee, Single-wall carbon nanotubes as attractive toughening agents in alumina-based nanocomposites, *Nat. Mater.* **2**, 38–42 (2003).
34. N. Jing, Q. Xue, C. Ling, M. Shan, T. Zhang, X. Zhou, and Z. Jiao, Effect of defects on Young's modulus of graphene sheets: a molecular dynamics simulation, *RSC Adv.* **2**, 9124–9129 (2012).
35. T. Kuilla, S. Bhadra, D. Yao, N. H. Kim, S. Bose, and J. H. Lee, Recent advances in graphene based polymer composites, *Prog. Polym. Sci.* **35**, 1350–1375 (2010).
36. T. K. Das and S. Prusty, Graphene-based polymer composites and their applications, *Polymer-Plastics Technol. Eng.* **52**, 319–331 (2013).
37. R. Verdejo, M. M Bernal, L. J Romasanta, and M. A. Lopaz-Manchado, Graphene filled polymer nanocomposites, *J. Mater. Chem.* **21**, 3301–3310 (2011).
38. J. H. Warner, F. Schaffel, A. Bachmatiuk, and M. H. Rummeli, *Graphene: Fundamentals and Emergent Applications*, 1st ed., Elsevier, New York (2012).
39. A. K. Geim and K. S. Novoselov, The rise of graphene, *Nat. Mater.* **6**, 183–191 (2007).
40. C. N. R. Rao, A. K. Sood, K. S. Subrahmanyam, and A. Govindaraj, Graphene: the new two-dimensional nanomaterial, *Angew. Chem. Int. Ed.* **48**, 7752–7777 (2009).
41. S. Park, R.S. Ruoff, Chemical methods for the production of graphenes, *Nat. Nanotechnol.*, DOI: 10.1038/NNANO.2009.58 (2009).
42. M. Taghioskoui, Trends in graphene research, *Mater. Today* **12**, 34–37 (2009).
43. P. Steurer, R. Wissert, R. Thomann, and R. Mulhaupt, Functionalized graphenes and thermoplastic nanocomposites based upon expanded graphite oxide, *Macromol. Rapid Commun.* **30**, 316–327 (2009).
44. C. Soldano, A. Mahmood, and E. Dujardin, Production, properties and potential of graphene, *Carbon* **48**, 2127–2150 (2010).
45. A. Shukla, R. Kumar, J. Mazher, and A. Balan, Graphene made easy: High quality, large-area samples, *Solid State Commun.* **149**, 718–721 (2009).
46. V. Singh, D. Joung, L. Zhai, S. Das, S. I Khondaker, and S. Seal, Graphene based materials: Past, present and future, *Prog. Mater. Sci.* **56**, 1178–1271 (2011).

47. A. A. Balandin, Thermal properties of graphene and nanostructured carbon materials, *Nat. Mater.* **10**, 569–581 (2011).
48. R. Cooper, B. D'Anjou, N. Ghattamaneni, B. Harack, M. Hilke, A. Horth, N. Majlis, M. Massicotte, L. Vandsburger, E. Whiteway, and V. Yu, Experimental review of graphene, *ISRN Condens. Matter Phys.* **501686** (56pp) (2012).
49. H. Wang, T. Maiyalagan, and X. Wang, Review on recent progress in nitrogen-doped graphene: synthesis, characterization, and its potential applications, *ACS Catal.* **2**, 781–794 (2012).
50. K. S. Novoselov, V. I. Fal'ko, L. Colombo, P. R. Gellert, M. G. Schwab, and K. Kim, A roadmap for graphene, *Nature* **490**, 192–200 (2012).
51. Q. Tang, Z. Zhou, and Z. Chen, Graphene-related nanomaterials: tuning properties by functionalization, *Nanoscale* **5**, 4541–4583 (2013).
52. Y. W. Sham and S. M. Notley, A review of fundamental properties and applications of polymer-graphene hybrid materials, *Soft Matter.* **9**, 6645–6653 (2013).
53. E. McCann and M. Koshino, The electronic properties of bilayer graphene, *Rep. Prog. Phys.* **76**, 056503 (2013).
54. K. Yang, L. Feng, X. Shi, and Z. Liu, Nano-graphene in biomedicine: theranostic applications, *Chem. Soc. Rev.* **42**, 530–547 (2013).
55. S. Z. Butler, S. M. Hollen, L. Cao, Y. Cui, J. A. Gupta, H. R. Gutierrez, T. F. Heinz, S. S. Hong, R. D. Robinson, R. S. Ruoff, S. Salahuddin, J. Shan, L. Shi, M. G. Spencer, M. Terrones, W. Windl, J. E. Goldberger, Progress. Challenges, and Opportunities in Two-Dimensional Materials beyond Graphene, *ACS Nano.* **7**(4), 2898–2926 (2013).
56. Y. Zhang, L. Zhang, and C. Zhou, Review of chemical vapor deposition of graphene and related applications, *Acc. Chem. Res.* **46**(10), 2329–2339 (2013).
57. R. K. Layek and A. K. Nandi, A review on synthesis and properties of polymer functionalized graphene, *Polymer* **54**, 5087–5103 (2013).
58. V. Dhand, K. Y Rhee, H. J. Kim, and D. H Jung, A comprehensive review of graphene nanocomposites: research status and trends, *J. Nanomater.* 763953 (2013).
59. W. Cummings, D. L Duong, V. L Nguyen, D. V Tuan, J. Kotakoski, J. E. B. Vargas, Y. H Lee, and S. Roche, Charge transport in polycrystalline graphene: challenges and opportunities, *Adv. Mater.* **26**, 5079–5094 (2014).
60. A. C. Ferrari, F. Bonaccorso, V. Falko, K. S. Novoselov, S. Roche, P. Boggild, S. Borini, F. H. L. Koppens, V. Palermo, N. Pugno, J. A. Garrido, R. Sordan, A. Bianco, L. Ballerini, M. Prato, E. Lidorikis, J. Kivioja, C. Marinelli, T. Ryhanen, A. Morpurgo, J. N. Coleman, V. Nicolosi, L. Colombo, A. Fert, M. Garcia-Hernandez, A. Bachtold, G. F. Schneider, F. Guinea, C. Dekker, M. Barbone, Z. Sun, C. Galiotis, A. N. Grigorenko, G. Konstantatos, A. Kis, M. Katsnelson, L. Vandersypen, A. Loiseau, V. Morandi, D. Neumaier, E. Treossi, V. Pellegrini, M. Polini, A. Tredicucci, G. M. Williams, B. H. Hong, Jong-Hyun Ahn, J. M. Kim, H. Zirath, B. J. van Wees, H. van der Zant, L. Occhipinti, A. D. Matteo, I. A. Kinloch, T. Seyller, E. Quesnel, X. Feng, K. Teo, N. Rupesinghe, P. Hakonen, S. R. T. Neil, Q. Tannock, T. Lofwander, J. Kinaret, Science and technology roadmap for graphene, related two-dimensional crystals, and hybrid systems, *Nanoscale*
61. X. Zhang, H. Zhang, C. Li, K. Wang, X. Sun, and Y. Ma, Recent advances in porous graphene materials for supercapacitor applications, *RSC Adv.* **4**, 45862–45884 (2014).
62. Editorial, Ten years in two dimensions, *Nat. Nanotechnol.* **9**, 725 (2014).
63. P. Randviir, D. A. C. Brownson, and C. E Banks, A decade of graphene research: production, application and outlook, *Mater. Today* **17**(9), 426–432 (2014).
64. K. S Novoselov, A. K Geim, S. V Morozov, D. Jiang, Y. Zhang, S. V Dubonos, I. V Grigorieva, and A. A Firsov, Electric field effect in atomically thin carbon films, *Science* **306**, 666–669 (2004).
65. U. K. Sur, Graphene: a rising star on the horizon of materials science, *Int. J. Electrochem.* 237689 (2012).
66. K. Geim, Graphene: status and prospects, *Science* **324**, 1530–1534 (2009).
67. L. Ma, J. Wang, and F. Ding, Recent progress and challenges in graphene nanoribbon synthesis, *ChemPhysChem.* **14**, 47–54 (2013).
68. Editorial, It's still all about graphene, *Nat. Mater.* **10**, 1 (2011).
69. R. Garg, N. K. Dutta, N. R. Choudhuri, Work function engineering of graphene, *Nanomaterials* **4**, 267–300 (2014).
70. F. Bonaccorso, A. Lombardo, T. Hasan, Z. Sun, L. Colombo, and A. C. Ferrari, Production and processing of graphene and 2d crystals, *Mater. Today* **15**(12), 564–589 (2012).
71. Y. L Zhong, Z. Tian, G. P Simon, and D. Li, Scalable production of graphene via wet chemistry: progress and challenges, *Mater. Today* **18**(2), 73–78 (2015).
72. M. I. Katsnelson, Graphene: carbon in two dimensions, *Mater. Today* **10**, 20–27 (2007).
73. J. C. Meyer, A. K. Geim, M. I. Katsnelson, K. S. Novoselov, T. J. Booth, and S. Roth, The structure of suspended graphene sheets, *Nature* **446**, 60–63 (2007).
74. N. Ye and P. Shi, Application of Graphene-Based Materials in Solid-Phase Extraction and Solid-Phase Microextraction, *Sep. Purif. Rev.* **44**, 183–198 (2015).
75. S. Gadipelli and Z. X Guo, Graphene-based materials: Synthesis and gas sorption, storage and separation, *Prog. Mater. Sci.* **69**, 1–16 (2015).
76. A. T. Lawal, Synthesis and utilization of graphene for fabrication of electrochemical sensors, *Talanta* **131**, 424–443 (2015).
77. Q. Fang, Y. Shen, and B. Chen, Synthesis, decoration and properties of three-dimensional graphene-based macrostructures: A review, *Chem. Eng. J.* **264**, 753–771 (2015).
78. P. T. Araujo, M. Terrones, and M. S. Dresselhaus, Defects and impurities in graphene-like materials, *Mater. Today* **15**(3), 98–109 (2012).
79. M. G Ahangari, Effect of defect and temperature on the mechanical and electronic properties of graphdiyne: a theoretical study, *Physica E* **66**, 140–147 (2015).
80. M. A. Bissett, S. Konabe, S. Okada, M. Tsuji, and H. Ago, Enhanced chemical reactivity of graphene induced by mechanical strain, *ACS Nano* **7**(11), 10335–10343 (2013).
81. O. Akhavan, The effect of heat treatment on formation of graphene thin films from graphene oxide nanosheets, *Carbon* **48**, 509–519 (2010).

82. B. W. Jeong, J. Ihm, and G. D. Lee, Stability of dislocation defect with two pentagon-heptagon pairs in graphene, *Phys. Rev. B Condens. Matter* **78**, 165403 (2008).
83. G. Compagnini, G. Forte, F. Giannazzo, V. Raineri, A. L. Magna, and I. Deretzis, Ion beam induced defects in graphene: Raman spectroscopy and DFT calculations, *J. Mol. Struct.* **993**, 506–509 (2011).
84. G. Compagnini, F. Giannazzo, S. Sonde, V. Raineri, and E. Rimini, Ion irradiation and defect formation in single layer graphene, *Carbon* **47**, 3201–3207 (2009).
85. J. Martinez-Asencio and M. J. Caturla, Molecular dynamics simulations of defect production in graphene by carbon irradiation, *Nucl. Instrum. Meth Phys. Res. Sect. B*; http://dx.doi.org/10.1016/j.nimb.2014.12.010 (2015).
86. Z. Jian, H. Ming, and Q. Feng, Effect of vacancy defects on the young's modulus and fracture strength of graphene: a molecular dynamics study, *Chin. J. Chem.* **30**, 1399–1404 (2012).
87. F. Banhart, J. Kotakoski, and A. V. Krasheninnikov, Structural defects in graphene, *ACS Nano* **5**, 26–41 (2011).
88. L. Liu, M. Qing, Y. Wang, and S. Chen, Defects in graphene: generation, healing, and their efeects on the properties of graphene: a review, *J. Mater. Sci. Technol.* **31**, 599–606 (2015).
89. T. Zhang, X. Li, and H. Gao, Designing graphene structure with controlled distributions of topological defects: A case study of toughness enhancement in graphene ruga, *Extreme Mech. Lett.* **1**, 3–8 (2014).
90. W. Robertson and J. H. Warner, Atomic resolution imaging of graphene by transmission electron microscopy, *Nanoscale Res. Lett.* **5**, 4079–4093 (2013).
91. L. Xu, N. Wei, and Y. Zheng, Mechanical properties of highly defective graphene: from brittle rupture to ductile fracture, *Nanotechnology* **24**, 505703 (2013).
92. S. Sun, C. Wang, M. Chen, and J. Zheng, A novel method to control atomic defects in graphene sheets, by selective surface reactions, *Appl. Surf. Sci.* **283**, 566–570 (2013).
93. J. Liu, Z. Liu, C. J. Barrow, and W. Yang, Molecularly engineered graphene surfaces for sensing applications: A review, *Anal. Chim. Acta* **859**, 1–19 (2015).
94. S. Yadav, Z. Zhu, and C. V. Singh, Defect engineering of graphene for effective hydrogen storage, *Int. J. Hydrog. Ener.* **39**, 4981–4995 (2014).
95. M. Terrones, A. R. Botello-Mendez, J. Campos-Delgado, F. Lopez-Urias, Y. I. Vega-Cantu, F. J. Rodriguez-Macias, A. L Elias, E. Munoz-Sandoval, A. G. Cano-Marquez, J. C Charlier, and H. Terrones, Graphene and graphite nanoribbons: Morphology, properties, synthesis, defects and applications, *Nano Today* **5**, 351–372 (2010).
96. X. Y Liu, J. M Zhang, K. W Xu, and V. Ji, Improving SO_2 gas sensing properties of graphene by introducing dopant and defect: A first-principles study, *Appl. Surf. Sci.* **313**, 405–410 (2014).
97. T. Li, X. Tang, Z. Liu, and P. Zhang, Effect of intrinsic defects on electronic structure of bilayer graphene: First-principles calculations, *Physica E* **43**, 1597–1601 (2011).
98. S. S. Terdalkar, S. Huang, H. Yuan, J. J. Rencis, T. Zhu, and S. Zhang, Nanoscale fracture in graphene, *Chem. Phys. Lett.* **494**, 218–222 (2010).
99. T. Zhu, J. Li, S. Ogata, and S. Yip, Mechanics of ultra-strength materials, *MRS Bull.* **34**, 167–172 (2009).
100. H. E. Troiani, M. Miki-Yoshida, G. A. Camacho-Bragado, M. A. L. Marques, A. Rubio, J. A. Ascencio, and M. Jose-Yacaman, Direct obsevation of the mechanical properties of single-walled carbon nanotubes and their junctions at the atomic level, *Nano Lett.* **3**, 751–755 (2003).
101. T. Dumitrica, T. Belytschko, and B. I. Yakobson, Bond-breaking bifurcation states in carbon nanotube fracture, *J. Chem. Phys.* **118**, 9485–9488 (2003).
102. T. Dumitrica, M. Hua, and B. I. Yakobson, Symmetry-, time-, and temperature-dependent strength of carbon nanotubes, *Proc. Natl. Acad. Sci. U.S.A.* **103**, 6105 (2006).
103. T. Dumitrica and B. I. Yakobson, Strain-rate and temperature dependent plastic yield in carbon nanotubes from ab initio calculations, *Appl. Phys. Lett.* **84**, 2775–2777 (2004).
104. M. B. Nardelli, B. I. Yakobson, and J. Bernholc, Brittle and ductile behavior in carbon nanotubes, *Phys. Rev. Lett.* **81**, 4656 (1998).
105. S. Zhang and T. Zhu, Atomic geometry and energetic of carbon nanotube necking, *Philos. Mag. Lett.* **87**, 567 (2007).
106. B.I. Yakobson, Mechanical relaxation and "intermolecular plasticity" in carbon nanotubes, *Appl. Phys. Lett.* **72**, 918–920 (1998).
107. J. Y. Huang, F. Ding, and B. I. Yakobson, Dislocation dynamics in multiwalled carbon nanotubes at high temperatures, *Phys. Rev. Lett.* **100**, 035503 (2008).
108. J. Y. Huang, S. Chen, S. H. Jo, Z. Wang, D. X Han, G. Chen, M. S Dresselhaus, and Z. F. Ren, Atomic-scale imaging of wall-by-wall breakdown and concurrent transport measurement in multiwall carbon nanotubes, *Phys. Rev. Lett.* **94**, 236802 (2005).
109. D. Bozovic, M. Bockrath, J. H. Hafner, C. M. Lieber, H. Park, and M. Tinkham, Plastic deformations in mechanically strained single-walled carbon nanotubes, *Phys. Rev. B Condens. Matter* **67**, 033407 (2003).
110. S. L Zhang, S. L Mielke, R. Khare, D. Troya, R. S Ruoff, G. C Schatz, and T. Belytschko, Mechanics of defects in carbon nanotubes: Atomistic and multiscale simulations, *Phys. Rev. B Condens. Matter* **71**, 115403 (2005).
111. R. A. Quinlan, M. Cai, R. A. Outlaw, S. M. Butler, J. R. Miller, and A. N. Mansour, Investigation of defects generated in vertically oriented graphene, *Carbon* **64**, 92–100 (2013).
112. X. Wei, B. Fragneaud, C. A Marianetti, and J. W Kysar, Nonlinear elastic behavior of graphene: Ab initio calculations to continuum description, *Phys. Rev. B Condens. Matter* **80**, 205407 (2009).
113. C. A. Marianetti, H.G. Yevick, Failure mechanisms of graphene under tension, *Phys. Rev. Lett.* **105**, 245502 (2010).
114. G. V. Lier, C. V. Alsenoy, V. V. Doren, and P. Geerlings, Ab initio study of the elastic properties of single-walled carbon nanotubes and graphene, *Chem. Phys. Lett.* **326**, 181–185 (2000).
115. E. Konstantinova, S. O. Dantas, and P. M. V. B. Barone, Electronic and elastic properties of two-dimensional carbon planes, *Phys. Rev. B Condens. Matter* **74**, 035417 (2006).
116. K. N. Kudin and G. E. Scuseria, C_2F, BN and C nanoshell elasticity from ab initio computations, *Phys. Rev. B: Condens. Matter* **64**, 235406 (2001).

117. Y. Wei, B. Wang, J. Wu, R. Yang, and M. L. Dunn, Bending rigity and Gaussian bending stiffness of single-layered graphene, *Nano Lett.* **13**, 26–30 (2013).
118. R. Faccio, P. A. Denis, H. Pardo, C. Goyenola, and A. W. Mombru, Mechanical properties of graphene nanoribbons, *J. Phys. Condens. Matter* **21**, 285304 (2009).
119. Y. S. Han and V. Tomar, An ab-initio investigation of the effect of graphene on the strength-electron density correlation in SiC grain boundaries, *Comput. Mater. Sci.* **92**, 422–430 (2014).
120. J. Zhao, H. Zeng, J. Wei, B. Li, and D. Xu, Atomistic simulations of divacancy defects in armchair graphene nanoribbons: Stability, electronic structure, and electron transport properties, *Phys. Lett. A* **378**, 416–420 (2014).
121. X. Qin, Q. Meng, Y. Feng, and Y. Gao, Graphene with line defects as a membrane for gas separation: Design via a first-principles modeling, *Surf. Sci.* **607**, 153–158 (2013).
122. L. Wu, T. Hou, Y. Li, K. S. Chan, and S. T. Lee, First-principles study on migration and coalescence of point defects in monolayer graphene, *J. Phys. Chem. C* **117**, 17066–17072 (2013).
123. A. Sakhaee-Pour, Elastic properties of single-layered graphene sheet, *Solid State Commun.* **149**, 91–95 (2009).
124. C. Baykasoglu and A. Mugan, Nonlinear fracture analysis of single-layer graphene sheets, *Eng. Fract. Mech.* **96**, 241–250 (2012).
125. C. Li and T. W. Chou, A structural mechanics approach for the analysis of carbon nanotubes, *Int. J. Solids Struct.* **40**, 2487–2499 (2003).
126. T. Chang and H. Gao, Size-dependent elastic properties of a single-walled carbon nanotube via a molecular mechanics model, *J. Mech. Phys. Solids* **51**, 1059–1074 (2003).
127. G. M. Odegard, T. S. Gates, L. M. Nicholson, and K. E. Wise, Equivalent-continuum modeling with application to carbon nanotubes, *NASA/TM-2002-211454*.
128. Y. Chandra, F. Scarpa, R. Chowdhury, S. Adhikari, and J. Sienz, Multiscale hybrid atomistic-FE approach for the nonlinear tensile behaviour of graphene nanocomposites, *Composites Part A* **46**, 147–153 (2013).
129. M. W. Roberts, C. B. Clemons, J. P. Wilber, G. W. Young, A. Buldum, and D. D. Quinn, Continuum plate theory and atomistic modeling to find the flexural rigidity of a graphene sheet interacting with a substrate, *Int. J. Nanotechnol.* **2010**, 868492 (2010).
130. H. S. Shen, L. Shen, and C. L. Zhang, Nonlocal plate model for nonlinear bending of single-layer graphene sheets subjected to transverse loads in thermal environments, *Appl. Phys. A* **103**, 103–112 (2011).
131. P. Joshi and S. H. Upadhyay, Evaluation of elastic properties of muti walled carbon nanotube reinforced composite, *Comput. Mater. Sci.* **81**, 332–338 (2014).
132. P. Joshi and S. H. Upadhyay, Effect of interphase on elastic behavior of multiwalled carbon nanotube reinforced composite, *Comput. Mater. Sci.* **87**, 267–273 (2014).
133. P. Joshi and S. H. Upadhyay, Analysis of alignment effect on carbon nanotube layer in nanocomposites, *Physica E* **66**, 221–227 (2015).
134. A. Parashar and P. Mertiny, Study of mode I fracture of graphene sheets using atomistic based finite element modeling and virtual crack closure technique, *Int. J. Fract.* **176**, 119–126 (2012).
135. A. Parashar and P. Mertiny, Multiscale model to investigate the effect of graphene on the fracture characteristics of graphene/polymer nanocomposites, *Nanoscale Res. Lett.* **7**, 595 (2012).
136. K. M. Liew, C. H. Wong, X. Q. He, M. J. Tan, and S. A. Meguid, Nanomechanics of single and multiwalled carbon nanotubes, *Phys. Rev. B Condens. Matter* **69**, 115429 (2004).
137. U. A. Joshi, S. C. Sharma, and S. P. Harsha, Effect of carbon nanotube orientation on the mechanical properties of nanocomposites, *Composites Part B* **43**, 2063–2071 (2012).
138. A. Y. Joshi, S. P. Harsha, and S. C. Sharma, Vibration signature analysis of single walled carbon nanotube based nanomechanical sensors, *Physica E* **42**, 2115–2123 (2010).
139. U. A. Joshi, S. C. Sharma, and S. P. Harsha, Effect of waviness on the mechanical properties of carbon nanotube based composites, *Physica E* **43**, 1453–1460 (2011).
140. U. A. Joshi, S. C. Sharma, and S. P. Harsha, A multiscale approach for estimating the chirality effects in carbon nanotube reinforced composites, *Physica E* **45**, 28–35 (2012).
141. K. I. Tserpes and P. Papanikos, Finite element modeling of single-walled carbon nanotubes, *Composites Part B* **36**, 468–477 (2005).
142. P. Papanikos, D. D. Nikolopoulos, and K. I. Tserpes, Equivalent beams for carbon nanotubes, *Comput. Mater. Sci.* **43**, 345–352 (2008).
143. F. Scarpa and S. Adhikari, A mechanical equivalence for Poisson's ratio and thickness of C-C bonds in single wall carbon nanotubes, *J. Phys. D Appl. Phys.* **41**, 085306 (2008).
144. F. Scarpa, S. Adhikari, and R. Chowdhury, The tranverse elasticity of bilayer graphene, *Phys. Lett. A* **374**, 2053–2057 (2010).
145. J. R. Xiao, B. A. Gama, and J. W. Gillespie Jr., An analytical molecular structural mechanics model for the mechanical properties of carbon nanotubes, *Int. J. Solids Struct.* **42**, 3075–3092 (2005).
146. A. Parashar and P. Mertiny, Effect of van der Waals interaction on the mode I fracture characteristics of graphene sheet, *Solid State Commun.* **173**, 56–60 (2013).
147. Y. Jin and F. G. Yuan, Nanoscopic modeling of fracture of 2D graphene systems, *J. Nanosci. Nanotechnol.* **5**, 601–608 (2005).
148. Y. Jin and F. G. Yuan, Atomic Simulations of J-integral in 2D Graphene Nanosystems, *J. Nanosci. Nanotechnol.* **5**, 2099–2107 (2005).
149. J. L. Tsai, S. H. Tzeng, and Y. J. Tzou, Characterizing the fracture parameters of a graphene sheet using atomistic simulation and continuum mechanics, *Int. J. Solids Struct.* **47**, 503–509 (2010).
150. M. A. N. Dewapriya, R. K. N. D. Rajapakse, and A. S. Phani, Atomistic and continuum modeling of temperature-dependent fracture of graphene, *Int. J. Fract.*, **187**, 199–212 (2014).
151. M. A. N. Dewapriya and R. K. N. D. Rajapakse, Effects of free edges and vacancy defects on the mechanical properties of graphene, *Proc. of the 14th IEEE International Conference on Nanotechnology Toronto, Canada* (2014).
152. M. A. N. Dewapriya, A. Srikantha Phani, and R. K. N. D. Rajapakse, Influence of temperature and free edges on the mechanical properties of graphene, *Model. Simul. Mater. Sci. Eng.* **21**, 065017 (2013).

153. M. A. N. Dewapriya and R. K. N. D. Rajapakse, Molecular dynamics simulations and continuum modeling of temperature and strain rate dependent fracture strength of graphene with vacancy defects, *J. Appl. Mech.* **81**, 081010 (2014).
154. Y. Gao and P. Hao, Mechanical properties of monolayer graphene under tensile and compressive loading, *Physica E* **41**, 1561–1566 (2009).
155. H. Zhao and N. R. Aluru, Temperature and strain-rate dependent fracture strength of graphene, *J. Appl. Phys.* **108**, 064321 (2010).
156. Y. Zheng, N. Wei, Z. Fan, L. Xu, and Z. Huang, Mechanical properties of grafold: a demonstration of strengthened graphene, *Nanotechnology* **22**, 405701 (2011).
157. Y. Y Zhang, Q. X Pei, and C. M Wang, Mechanical properties of graphynes under tension: A molecular dynamics study, *Appl. Phys. Lett.* **101**, 081909 (2012).
158. L. Wang and Q. Zhang, Elastic behavior of bilayer graphene under in-plane loadings, *Curr. Appl. Phys.* **12**, 1173–1177 (2012).
159. Q. Lu, W. Gao, and R. Huang, Atomistic simulation and continuum modeling of graphene nanoribbons under uniaxial tension, *Model. Simul. Mater. Sci. Eng.* **19**, 054006 (2011).
160. L. Zhou, Y. Wang, and G. Cao, Elastic properties of monolayer graphene with different chiralities, *J. Phys. Condens. Matter* **25**, 125302 (2013).
161. L. Zhou, Y. Wang, and G. Cao, van der Waals effect on the nanoindentation response of free standing monolayer graphene, *Carbon* **57**, 357–362 (2013).
162. L. Zhou, Y. Wang, and G. Cao, Boundary condition and pre-strain effects on the free standing indentation response of graphene monolayer, *J. Phys. Condens. Matter* **25**, 475303 (2013).
163. L. Zhou, J. Xue, Y. Wang, and G. Cao, Molecular mechanics simulations of the deformation mechanism of graphene monolayer under free standing indentation, *Carbon* **63**, 117–124 (2013).
164. L. Zhou, Y. Wang, and G. Cao, Estimating the elastic properties of few-layer graphene from the free-standing indentation response, *J. Phys. Condens. Matter* **25**, 475301 (2013).
165. A. Sakhaee-Pour, M. T. Ahmadian, and R. Naghdabadi, Vibrational analysis of single-layered graphene sheets, *Nanotechnology* **19**, 085702 (2008).
166. A. Sakhaee-Pour, Elastic buckling of single-layered graphene sheet, *Comput. Mater. Sci.* **45**, 266–270 (2009).
167. Z. Lu and M. L. Dunn, van der Waals adhesion of graphene membranes, *J. Appl. Phys.* **107**, 044301 (2010).
168. Q. Wang, Simulations of the bending rigidity of graphene, *Phys. Lett. A* **374**, 1180–1183 (2010).
169. M. Neek-Amal and F. M. Peeters, Graphene nanoribbons subjected to axial stress, *Phys. Rev. B Condens. Matter* **82**, 085432 (2010).
170. K. Min and N. R. Aluru, Mechanical properties of graphene under shear deformation, *Appl. Phys. Lett.* **98**, 013113 (2011).
171. P. Liu and Y. W. Zhang, A theoretical analysis of frictional and defect characteristics of graphene probed by a capped single-walled carbon nanotube, *Carbon* **49**, 3687–3697 (2011).
172. S. Sharma, R. Chandra, P. Kumar, and N. Kumar, Effect of Stone-Wales and vacancy defects on elastic moduli of carbon nanotubes and their composites using molecular dynamics simulation, *Comput. Mater. Sci.* **86**, 1–8 (2014).
173. J. W. Kang, H. W. Kim, K. S. Kim, and J. H. Lee, Molecular dynamics modeling and simulation of a graphene-based nano electromechanical resonator, *Curr. Appl. Phys.* **13**, 789–794 (2013).
174. S. P. Kiselev and E. V. Zhirov, Molecular dynamics simulation of deformation and fracture of graphene under uniaxial tension, *Phys. Mesomech.* **16**(2), 1–8 (2013).
175. W. Wang, S. Li, J. Min, C. Yi, Y. Zhan, and M. Li, Nanoindentation experiments for single-layer rectangular graphene films: a molecular dynamics study, *Nanoscale Res. Lett.* **9**(41), 1–8 (2014).
176. E. Cadelano, P. L. Palla, S. Giordano, and L. Colombo, Nonlinear elasticity of monolayer graphene, *Phys. Rev. Lett.* **102**, 235502 (2009).
177. J. N. B. Rodrigues, P. A. D. Goncalves, N. F. G. Rodrigues, R. M. Ribeiro, J. M. B. Lopes dos Santos, and N. M. R. Peres, Zigzag graphene nanoribbon edge reconstruction with Stone-Wales defects, *Phys. Rev. B Condens. Matter* **84**, 155435 (2011).
178. E. B. Tadmor and R. E. Miller, *Modeling Materials Continuum, Atomistic and Multiscale Techniques*, 1st ed., Cambridge University Press, New York (2011).
179. W. Jiang, J. S. Wang, and B. Li, Young's modulus of Graphene: a molecular dynamics study, *Phys. Rev. B Condens. Matter* **80**, 113405 (2009).
180. J. L. Tsai and J. F. Tu, Characterizing mechanical properties of graphite using molecular dynamics simulation, *Mater. Des.* **31**, 194–199 (2010).
181. M. Neek-Amal and F. M. Peeters, Linear reduction of stiffness and vibration frequencies in defected circular monolayer graphene, *Phys. Rev. B Condens. Matter* **81**, 235437 (2010).
182. Z. Ni, H. Bu, M. Zou, H. Yi, K. Bi, and Y. Chen, Anisotropic mechanical properties of graphene sheets from molecular dynamics, *Physica B* **405**, 1301–1306 (2010).
183. R. Ansari, B. Motevalli, A. Montazeri, and S. Ajori, Fracture analysis of monolayer graphene sheets with double vacancy defects via MD simulation, *Solid State Commun.* **151**, 1141–1146 (2011).
184. Y. Y. Zhang and Y. T. Gu, Mechanical properties of graphene: Effects of layer number, temperature and isotope, *Comput. Mater. Sci.* **71**, 197–200 (2013).
185. H. Bu, Y. Chen, M. Zou, H. Yi, K. Bi, and Z. Ni, Atomistic simulations of mechanical properties of graphene nanoribbons, *Phys. Lett. A* **373**, 3359–3362 (2009).
186. H. Zhao, K. Min, and N. R. Aluru, Size and chirality dependent elastic properties of graphene nanoribbons under uniaxial tension, *Nano Lett.* **9**, 3012–3015 (2009).
187. W. Cai, J. Li, and S. Yip, Molecular dynamics, comprehensive nuclear materials, **1**, 249–265 (2012).
188. W. G. Hoover, Canonical dynamics: Equilibrium phase-space distributions, *Phys. Rev. A At. Mol. Opt. Phys.* **31**, 1695–1697 (1985).
189. S. Nose, A uniform formulation of the constant temperature molecular dynamics methods, *J. Chem. Phys.* **81** (1), 511–549 (1984).

190. M. P. Allen, D. J. Tildesley, and R. Allen, *Computer Simulation of Liquids*, Oxford University Press, New York (1988).
191. Q. X. Pei, Y. W. Zhang, and V. B. Shenoy, A molecular dynamics study of the mechanical properties of hydrogen functionalized graphene, *Carbon* **48**, 898–904 (2010).
192. N. Chandra, S. Namilae, and C. Shet, Local elastic properties of carbon nanotubes in the presence of Stone-Wales defects, *Phys. Rev. B Condens. Matter* **69**, 094101 (2004).
193. Y. Huang, J. Wu, and K. C. Hwang, Thickness of graphene and single-wall carbon nanotubes, *Phys. Rev. B Condens. Matter* **74**, 245413 (2006).
194. D. W. Brenner, O. A. Shenderova, J. A. Harrison, S. J. Stuart, B. Ni, and S. B. Sinnott, A second-generation reactive empirical bond order (REBO) potential energy expression for hydrocarbons, *J. Phys. Condens. Matter* **14**, 783–802 (2002).
195. S. J. Stuart, A. B. Tutein, and J. A. Harrison, A reactive potential for hydrocarbons with intermolecular interactions, *J. Chem. Phys.* **112**(14), 6472–6486 (2000).
196. L. He, S. Guo, J. Lei, Z. Sha, and Z. Liu, The effect of Stone-Thrower-Wales defects on mechanical properties of graphene sheets – A molecular dynamics study, *Carbon* **75**, 124–132 (2014).
197. J. Wu and Y. Wei, Grain misorintation and grain-boundary rotation dependent mechanical properties of polycrystalline graphene, *J. Mech. Phys. Solids* **61**, 1421–1432 (2013).
198. Y. I. Jhon, S. E. Zhu, J. H. Ahn, and M. S. Jhon, The mechanical responses of tilted and non-tilted grain boundaries in graphene, *Carbon* **50**, 3708–3716 (2012).
199. Y. Zhang and C. Pan, Measurement of mechanical properties and number of layers of graphene from nano-indentation, *Diamond Relat. Mater.* **24**, 1–5 (2012).
200. D. Porezag, Th. Frauenheim, and Th. Kohler, Construction of tight-binding-like potentials on the basis of density-fuctional theory: Application to carbon, *Phys. Rev. B Condens. Matter* **51**, 12947–12957 (1995).
201. H. Sun, COMPASS: An ab initio force-field optimized for condensed-phase applications-overview with details on alkane and benzene compounds, *J. Phys. Chem. B* **102**, 7338–7364 (1998).
202. C. G. Navarro, M. Burghard, and K. Kern, Elastic properties of chemically derived single graphene sheets, *Nano Lett.* **8**, 2045–2049 (2008).
203. R. Rasuli, A. Iraji zad, and M. M. Ahadian, Mechanical properties of graphene cantilever from atomic force microscopy and density functional theory, *Nanotechnology* **21**, 185503 (2010).
204. J. W. Suk, R. D. Piner, J. An, and R. S. Ruoff, Mechanical properties of monolayer graphene oxide, *ACS Nano* **4**, 6557–6564 (2010).
205. H. M. Chien, M. C. Chuang, H. C. Tsai, H. W. Shiu, L. Y. Chang, C. H. Chen, S. W. Lee, J. D. White, and W. Y. Woon, On the nature of defects created on graphene by scanning probe lithography under ambient conditions, *Carbon* **80**, 318–324 (2014).
206. A. Gao, E. Zoethout, J. M. Sturm, C. J. Lee, and F. Bijkerk, Defect formation in single layer graphene under extreme ultraviolet irradiation, *Appl. Surf. Sci.* **317**, 745–751 (2014).
207. G. Imamura and K. Saiki, UV-irradiation induced defect formation on graphene on metals, *Chem. Phys. Lett.* **587**, 56–60 (2013).
208. C. Lee, X. Wei, J. W. Kysar, and J. Hone, Measurement of the elastic properties and intrinsic strength of monolayer graphene, *Science* **321**, 38–388 (2008).
209. I. W. Frank, D. M. Tanenbaum, A. M. van der Zande, and P. L. McEuen, Mechanical properties of suspended graphene sheets, *J. Vac. Sci. Technol. B* **25**, 2558–2561 (2007).
210. L. Shen, H. S. Shen, and C. L. Zhang, Temperature-dependent elastic properties of single layer graphene sheets, *Mater. Des.* **31**, 4445–4449 (2010).
211. A. Parashar and P. Mertiny, Representative volume element to estimate buckling behavior of graphene/polymer nanocomposite, *Nanoscale Res. Lett.* **7**, 515 (2012).
212. W. Wang, C. Shen, S. Li, J. Min, and C. Yi, Mechanical properties of single layer graphene nanoribbons through bending experimental simulations, *AIP Adv.* **4**, 031333 (2014).
213. C. D. Reddy, S. Rajendran, and K. M. Liew, Equilibrium configuration and continuum elastic properties of finite sized graphene, *Nanotechnology* **17**, 864–870 (2006).
214. A. G. Kvashnin, P. B. Sorokin, and D. G. Kvashnin, The theoretical study of mechanical properties of graphene membranes, *Fullerenes Nanotubes Carbon Nanostruct.* **18**, 497–500 (2010).
215. M. M. Shokrieh and R. Rafiee, Prediction of Young's modulus of graphene sheets and carbon nanotubes using nanoscale continuum mechanics approach, *Mater. Des.* **31**, 790–795 (2010).
216. J. R. Xiao, J. Staniszewski, and J. W. Gillespie Jr., Fracture and progressive failure of defective graphene sheets and carbon nanotubes, *Compos. Struct.* **88**, 602–609 (2009).
217. S. K. Georgantzinos, G. I. Giannopoulos, and N. K. Anifantis, Numerical investigation of elastic mechanical properties of graphene structures, *Mater. Des.* **31**, 4646–4654 (2010).
218. M. Canadija, M. Brcic, and J. Brnic, Bending behavior of single-layerd graphene nanosheets with vacancy defects, *Eng. Rev.* **33**, 09–14 (2013).
219. A. Tapia, R. Peon-Escalante, C. Villanueva, and F. Aviles, Influence of vacancies on the elastic properties of a graphene sheet, *Comput. Mater. Sci.* **55**, 255–262 (2012).
220. B. Mortazavi, O. Benzerara, H. Meyer, J. Bardon, and S. Ahzi, Combined molecular dynamics-finite element multiscale mdeling of thermal conduction in graphene epoxy nanocomposites, *Carbon* **60**, 356–365 (2013).
221. Y. Chandra, R. Chowdhury, F. Scarpa, S. Adhikari, J. Sienz, C. Arnold, T. Murmu, and D. Bould, Vibration frequency of graphene based composites: A multiscale approach, *Mater. Sci. Eng. B* **177**, 303–310 (2012).
222. S. Gupta, K. Dharamvir, and V. K. Jindal, Elastic moduli of single-walled carbon nanotubes and their ropes, *Phys. Rev. B Condens. Matter* **72**, 165428 (2005).
223. B. WenXing, Z. ChangChun, and C. WanZhao, Simulation of Young's modulus of single-walled carbon nanotubes by molecular dynamics, *Physica B* **352**, 156–163 (2004).
224. A. Hemmasizadeh, M. Mahzoon, E. Hadi, and R. Khandan, A method for developing the equivalent continuum model of a single layer graphene sheet, *Thi Solid Films* **516**, 7636–7640 (2008).
225. M. Neek-Amal and F. M. Peeters, Nanoindentation of a circular sheet of bilayer graphene, *Phys. Rev. B Condens. Matter* **81**, 235421 (2010).

226. F. Liu, P. Ming, and J. Li, Ab initio calculation of strength and phonon instability of graphene under tension, *Phys. Rev. B Condens. Matter* **76**, 064120 (2007).
227. D. Sanchez-Portal, E. Artacho, and J. M. Soler, Ab initio structural, elastic, and vibrational properties of carbon nanotubes, *Phys. Rev. B Condens. Matter* **59** (19), 12678–12688 (1999).
228. E. Hernandez, C. Goze, P. Bernier, and A. Rubio, Elastic properties of C and $B_xC_yN_z$ composite nanotubes, *Phys. Rev. Lett.* **80** (20), 4502–4505 (1998).
229. M. Meo and M. Rossi, Prediction of Young,s modulus of single wall carbon nanotubes by molecular-mechanics based finite element modeling, *Compos. Sci. Technol.* **66**, 1597–1605 (2006).
230. E. Bitzek, P. Gumbsch, Mechanisms of dislocation multiplication at crack tips, *Acta Mater.*, **61**, 1394–1403 (2013).
231. S. A. Niaki, J. R. Mianroodi, M. Sadeghi, and R. Naghdabadi, Dynamic and static fracture analyses of graphene sheets and carbon nanotubes, *Compos. Struct.* **94**, 2365–2372 (2012).
232. Y. G. Yanovsky, Y. N. Karnet, E. A. Nikitina, and S. M. Nikitin, Quantum mechanics study of the mechanism of deformation and fracture of graphene, *Phys. Mesomech.* **12**, 254–262 (2009).
233. S. K. Georgantzinos, D. E. Katsareas, and N. K. Anifantis, Limit load analysis of graphene with pinhole defects: A nonlinear structural mechanics approach, *Int. J. Mech. Sci.* **55**, 85–94 (2012).
234. Z. Xu, Graphene nano-ribbons under tension, *J. Computat. Theoret. Nanoscience* **6**, 1–3 (2009).
235. N. Wei, L. Xu, H. Q. Wang, and J. C. Zheng, Strain engineering of thermal conductivity in graphene sheets and nanoribbons: a demonstration on magic flexibility, *Nanotechnology* **22**, 105705 (2011).
236. L. Lindsay, W. Li, J. Carrete, N. Mingo, D. A. Broido, and T. L. Reinecke, Phonon thermal transport in strained and unstrained graphene from first principles, *Phys. Rev. B Condens. Matter* **89**, 155426 (2014).
237. J. Huang and C. H. Wong, Thickness, chirality and pattern dependence of elastic properties of hydrogen functionalized graphene, *Comput. Mater. Sci.* **92**, 192–198 (2014).
238. Q. X. Pei, Z. D. Sha, and Y. W. Zhang, A theoretical analysis of the thermal conductivity of hydrogenated graphene, *Carbon* **49**, 4752–4759 (2011).
239. W. X. Huang, Q. X. Pei, Z. S. Liu, and Y. W. Zhang, Thermal conductivity of fluorinated graphene: A non-equilibrium molecular dynamics study, *Chem. Phys. Lett.* **552**, 97–101 (2012).
240. Y. Y. Zhang, Q. X. Pei, and C. M. Wang, A molecular dynamics investigation on thermal conductivity of graphynes, *Comput. Mater. Sci.* **65**, 406–410 (2012).
241. D. Konatham, D. V. Papavassiliou, and A. Striolo, Thermal boundary resistance at the graphene-graphene interface estimated by molecular dynamics simulations, *Chem. Phys. Lett.* **527**, 47–50 (2012).
242. T. Ouyang, Y. Chen, Y. Xie, G. M. Stocks, and J. Zhong, Thermal conductance modulator based on folded graphene nanoribbons, *Appl. Phys. Lett.* **99**, 233101 (2011).
243. K. Kim, V. I. Artyukhov, W. Regan, Y. Liu, M. F. Crommie, B. I. Yakobson, and A. Zettl, Ripping graphene: preferred directions, *Nano Lett.* **12**, 293–297 (2012).
244. U. Ray and G. Balasubramanian, Reduced thermal conductivity of isotope substituted carbon nanomaterials: Nanotube versus graphene nanoribbons, *Chem. Phys. Lett.* **599**, 154–158 (2014).
245. S. Ghosh, W. Z. Bao, D. L. Nika, S. Subrina, E. P. Pokatilov, C. N. Lau, and A. A. Balandin, Dimensional crossover of thermal transport in few-layer graphene, *Nat. Mater.* **9**, 555–558 (2010).
246. S. Chen, A. L. Moore, W. Cai, J. W. Suk, J. An, C. Mishra, C. Amos, C. W. Magnuson, J. Kang, L. Shi, and R. S. Ruoff, Raman measurement of thermal transport in suspended monolayer graphene of variable sizes in vacuum and gaseous environments, *ACS Nano* **5**, 321–328 (2011).
247. A. A. Balandin, Thermal properties of graphene and nanostructured carbon materials, *Nat. Mater.* **10**, 569–581 (2011).
248. S. Chen, Q. Wu, C. Mishra, J. Kang, H. Zhang, K. Cho, W. Cai, A. A. Balandin, R. S. Ruoff, Thermal conductivity of isotopically modified graphene, *Nat. Mater.* **11**, 203–207 (2012).
249. D. Yang, F. Ma, Y. Sun, T. Hu, and K. Xu, Influence of typical defects on thermal conductivity of graphene nanoribbons: An equilibrium molecular dynamic simulation, *Appl. Surf. Sci.* **258**, 9926–9931 (2012).
250. B. Mortazavi and S. Ahzi, Thermal conductivity and tensile response of defective graphene: A molecular dynamics study, *Carbon* **63**, 460–470 (2013).
251. F. Hao, D. Fang, and Z. Xu, Mechanical and thermal transport properties of graphene with defects, *Appl. Phys. Lett.* **99**, 041901 (2011).
252. S. P. Wang, J. G. Guo, and L. J. Zhou, Influence of Stone-Wales defects on elastic properties of graphene nanofilms, *Physica E* **48**, 29–35 (2013).
253. B. Fan, X. B. Yang, and R. Zhang, Anisotropic mechanical properties and Stone-Wales defects in graphene monolayer: A theoretical study, *Phys. Lett. A* **374**, 2781–2784 (2010).
254. Z. G. Fthenakis, Z. Zhu, and D. Tomanek, Effect of structural defects on the thermal conductivity of graphene: From point to line defects to haeckelites, *Phys. Rev. B Condens. Matter* **89**, 125421 (2014)
255. T. Y. Ng, J. J. Yeo, and Z. S. Liu, A molecular dynamics study of the thermal conductivity of graphene nanoribbons containing dispersed Stone-Thrower-Wales defects, *Carbon* **50**, 4887–4893 (2012).
256. M. Hjort and S. Stafstrom, Modeling vacancies in graphite via the Huckel method, *Phys. Rev. B Condens. Matter* **61**, 14089–14094 (2000).
257. Y. Kim, J. Ihm, E. Yoon, and G. D. Lee, Dynamics and stability of divacancy defects in graphene, *Phys. Rev. B Condens. Matter* **84**, 075445 (2011).
258. G. D. Lee, C. Wang, E. Yoon, N. M. Hwang, D. Y. Kim, and K. Ho, Diffusion, coalescence, and reconstruction of vacancy defects in graphene layers, *Phys. Rev. Lett.* **95**, 205501 (2005).
259. J. Kotakoski, J. Meyer, S. Kurasch, D. Santos-Cottin, U. Kaiser, and A. Krasheninnikov, Stone-Wales-type transformation in carbon nanostructures driven by electron irradiation, *Phys. Rev. B Condens. Matter* **83**, 245420 (2011).
260. I. Zsoldos, Effect of topological defects on graphene geometry and stability, *Nanotechnol. Sci. Applic.* **3**, 101–106 (2010).

261. A. A. EI-Barbary, R. H. Telling, C. P. Ewels, M. I. Heggie, and P. R. Briddon, Structure and energetic of the vacancy in graphite, *Phys. Rev. B Condens. Matter* **68**, 144107 (2003).
262. A. Ito and S. Okamoto, Molecular dynamics analysis on effects of vacancies upon mechanical properties of graphene and graphite, *Eng. Lett.* **20**:3, EL_20_3_09.
263. A. Hashimoto, K. Suenaga, A. Gloten, K. Urita, and S. Iijima, Direct evidence for atomic defects in graphene layers, *Nature* **430**, 870–873 (2004).
264. Y. Yang, Mechanical properties of graphene with vacancy defects, *Res. Mater. Sci.* **2**(4), 50–57 (2013).
265. A. Santana, A. M. Popov, and E. Bichoutskaia, Stability and dynamics of vacancy in graphene flakes: Edge effects, *Chem. Phys. Lett.* **557**, 80–87 (2013).
266. J. Kotakoski and J. C. Meyer, Mechanical properties of polycrystalline graphene based on a realistic atomistic model, *Phys. Rev. B Condens. Matter* **85**, 195447 (2012).
267. Y. Y. Zhang, Y. Cheng, Q. X. Pei, C. M. Wang, and Y. Xiang, Thermal conductivity of defective graphene, *Phys. Lett. A* **376**, 3668–3672 (2012).
268. F. Hao, D. N. Fang, and Z. P. Xu, Mechanical and thermal transport properties of graphene with defects, *Appl. Phys. Lett.* **99**, 041901 (2011).
269. C. Sevik, H. Sevincli, G. Cuniberti, and T. Cagin, Phonon engineering in carbon nanotubes by controlling defect concentration, *Nano Lett.* **11**, 4971–4977 (2011).
270. H. Yang, Y. Tang, Y. Liu, X. Yu, and P. Yang, Thermal conductivity of graphene nanoribbons with defects and nitrogen doping, *React. Funct. Polym.* **79**, 29–35 (2014).
271. E. T. Swartz and R. O. Pohl, Thermal boundary resistance, *Rev. Mod. Phys.* **61**, 605–668 (1989).
272. D. Liu, P. Yang, X. Yuan, J. Guo, and N. Liao, The defect location effect on thermal conductivity of graphene nanoribbons based on molecular dynamics, *Phys. Lett. A* **379**, 810–814 (2014).
273. S. Ogata and Y. Shibutani, Ideal tensile strength and band gap of single-walled carbon nanotubes, *Phys. Rev. B Condens. Matter* **68**, 165409 (2003).
274. L. L. Bonilla and A. Carpio, Driving dislocations in graphene, *Science* **337**, 161–162 (2012).
275. O. V. Yazyev and S. G. Louie, Topological defects in graphene: Dislocations and grain boundaries, *Phys. Rev. B Condens. Matter* **81**, 195420 (2010).
276. J. H. Warner, E. R. Margine, M. Mukai, A. W. Robertson, F. Giustino, and A. I. Kirklandd, Dislocation-driven deformations in graphene, *Science* **337**, 209–212 (2012).
277. G. D. Lee, E. Yoon, N. M. Hwang, C. Zhuang, and K. M. Ho, Formation and development of dislocation in graphene, *Appl. Phys. Lett.* **102**, 021603 (2013).
278. B. Butz, C. Dolle, F. Niekiel, K. Weber, D. Waldmann, H. B. Weber, B. Meyer, and E. Spiecker, Dislocations in bilayer graphene, *Nature* **505**, 533 (2014).
279. M. P. Ariza, M. Ortiz, and R. Serrano, Long-term dynamic stability of discrete dislocations in graphene at finite temperature, *Int. J. Fract.* **166**, 215–223 (2010).
280. A. Carpio, L. L. Bonilla, F. de Juan, and M. A. H. Vozmediano, Dislocations in graphene, *New J. Phys.* **10**, 053021 (2008).
281. P. Nemes-Incze, K. J. Yoo, L. Tapaszto, G. Dobrik, J. Labar, Z. E. Horvath, C. Hwang, and L. P. Biro, Revealing the grain structure of graphene grown by chemical vapor deposition, *Appl. Phys. Lett.* **99**, 023104 (2011).
282. H. I. Rasool, C. Ophus, W. S. Klug, A. Zettl, and J. K. Gimzewski, Measurement of the intrinsic strength of crystalline and polycrystalline graphene, *Nature Commun.* **4**, 2811 (2013).
283. P. Xu, D. Qi, J. K. Schoelz, J. Thompson, P. M. Thibado, V. D. Wheeler, L. O. Nyakiti, R. L. Myers-Ward, C. R. Eddy Jr., D. K. Gaskill, M. Neek-Amal, and F. M. Peeters, Multilayer graphene, Moire patterns, grain boundaries and defects identified by scanning tunneling microscopy on the m-plane, non-polar surface of SiC, *Carbon* **80**, 75–81 (2014).
284. C. S. Ruiz-Vargas, H. L. Zhuang, P. Y. Huang, A. M. van der Zande, S. Garg, P. L. McEuen, D. A. Muller, R. G. Hennig, and J. Park, Softened elastic response and unzipping in chemical vapor deposition graphene membranes, *Nano Lett.* **11**, 2259–2263 (2011).
285. T. H. Liu, C. W. Pao, and C. C. Chang, Effects of dislocation densities and distributions on graphene grain boundary failure strengths from atomistic simulations, *Carbon* **50**, 3465–3472 (2013).
286. L. Yi, Z. Yin, Y. Zhang, and T. Chang, A theoretical evaluation of the temperature and strain-rate dependent fracture strength of tilt grain boundaries in graphene, *Carbon* **51**, 373–380 (2013).
287. M. Q. Chen, S. S. Quek, Z. D. Sha, C. H. Chiu, Q. X. Pei, and Y. W. Zhang, Effect of grain size, temperature and strain rate on the mechanical properties of polycrystalline graphene – A molecular dynamics study, *Carbon* **85**, 135–146 (2015).
288. J.R. Yin, W. H. Wu, W. Xie, Y. H. Ding, and P. Zhang, Influence of line defects on relaxation properties of graphene: A molecular dynamics stydy, *Physica E* **68**, 102–106 (2015).
289. F. Hao and D. Fang, Mechanical deformation and fracture mode of polycrystalline graphene: Atomistic simulations, *Phys. Lett. A* **376**, 1942–1947 (2012).
290. K. Zhang, J. Zhao, and J. P. Lu, Intrinsic strength and failure behaviors of graphene grain boundaries, *ACS Nano* **6**, 2704–2711 (2012).